

MicroRNA 200c and its effects on breast cancer  
and chemotherapy in a xenograft model

von Elisa Sophie Hörterer

Inaugural-Dissertation zur Erlangung der Doktorwürde  
der Tierärztlichen Fakultät der Ludwig-Maximilians-  
Universität München

**MicroRNA 200c and its effects on breast cancer and  
chemotherapy in a xenograft model**

von Elisa Sophie Hörterer

aus Traunstein

München 2022



Aus dem Veterinärwissenschaftlichen Department der Tierärztlichen Fakultät  
der Ludwig-Maximilians-Universität München

Lehrstuhl für Molekulare Tierzucht und Biotechnologie

Arbeit angefertigt unter der Leitung von: Univ.-Prof. Dr. Eckhard Wolf

Angefertigt am: Lehrstuhl für Pharmazeutische Biotechnologie, Fakultät für  
Chemie und Pharmazie der Ludwig-Maximilians-Universität München

Mentor: Univ.-Prof. Dr. Ernst Wagner



Gedruckt mit Genehmigung der Tierärztlichen Fakultät  
der Ludwig-Maximilians-Universität München

**Dekan:** Univ.-Prof. Dr. Reinhard K. Straubinger, Ph.D.

**Berichterstatter:** Univ.-Prof. Dr. Eckhard Wolf

**Korreferent:** Univ.-Prof. Dr. Johannes Hirschberger

**Tag der Promotion:** 12.02.2022



Für Adi und Theo



## TABLE OF CONTENTS

<b>I</b>	<b>INTRODUCTION .....</b>	<b>1</b>
<b>1</b>	<b>The microRNA family .....</b>	<b>2</b>
1.1	MiRNAs in physiological and pathological processes .....	3
1.2	MiR-200c and its influence on tumor cells .....	5
1.3	Inducible miR-200c in breast cancer cells .....	8
1.4	Therapeutic use of miRNAs .....	9
1.4.1	Obstacles of miRNA delivery .....	10
1.4.2	Sequence-defined oligoaminoamides .....	10
1.4.3	Shielding components .....	12
1.4.4	Targeting components .....	13
<b>2</b>	<b>Aims of the thesis .....</b>	<b>15</b>
<b>II</b>	<b>MICE, MATERIALS AND METHODS .....</b>	<b>17</b>
<b>1</b>	<b>Mice .....</b>	<b>17</b>
1.1	Mouse strain .....	17
1.2	Housing conditions .....	17
1.3	Health monitoring .....	18
<b>2</b>	<b>Materials .....</b>	<b>18</b>
2.1	Cell culture .....	18
2.2	Polyplexes .....	19
2.3	Nucleic acids and compounds .....	19
2.4	Animal treatment equipment .....	20
2.5	Doxycycline feed .....	20
2.6	Instruments .....	20
2.7	Software .....	21
<b>3</b>	<b>Methods .....</b>	<b>21</b>
3.1	Cell culture .....	21
3.2	<i>In vivo</i> experiments .....	21
3.2.1	Effect of miR-200c on tumor formation and growth .....	22
3.2.2	Influence of doxycycline on tumor growth .....	23
3.2.3	Intratumoral application of polyplexes .....	23
3.2.4	Antitumoral effects of miR-200c and doxorubicin .....	24
3.2.5	Bioimaging as validation of tumor absence .....	27
3.3	Statistical analysis .....	27
<b>III</b>	<b>RESULTS .....</b>	<b>29</b>

## Table of Contents

---

1	Effect of miR-200c on tumor formation and growth .....	29
2	Influence of doxycycline on tumor growth .....	34
3	Intratumoral application of polyplexes.....	37
4	Antitumoral effects of miR-200c and doxorubicin .....	38
<b>IV</b>	<b>DISCUSSION .....</b>	<b>53</b>
1	Effect of miR-200c on tumor formation and growth .....	53
2	Delivery of miR-200c .....	55
3	Antitumoral effects of miR-200c and doxorubicin .....	56
<b>V</b>	<b>SUMMARY .....</b>	<b>59</b>
<b>VI</b>	<b>ZUSAMMENFASSUNG .....</b>	<b>61</b>
<b>VII</b>	<b>REFERENCES .....</b>	<b>63</b>
<b>VIII</b>	<b>APPENDIX .....</b>	<b>71</b>
1	Publications.....	71
2	Posters.....	71
<b>IX</b>	<b>ACKNOWLEDGEMENTS .....</b>	<b>73</b>

## ABBREVIATIONS

°C	degree Celsius
µg, µl	microgram(s), microliter(s)
AGO protein	Argonaute protein
approx.	approximately
Bmi1	B cell-specific Moloney murine leukemia virus integration site
CO <sub>2</sub>	carbon dioxide
ctrl	control
dB	decibel
DBCO	dibenzocyclooctyne
DGCR8	DiGeorge syndrome critical region 8
DNA	deoxyribonucleic acid
e.g.	exempli gratia (for example)
EG5	eglin 5, kinesin spindle protein
EGFR	epidermal growth factor receptor
EMT	epithelial to mesenchymal transition
EPR effect	enhanced permeability and retention effect
equiv.	equivalent(s)
<i>et al.</i>	<i>et alii</i> (and others)
EXP-5	exportin-5
FCS	fetal calf serum
FLNA/FLNB	Filamin A/B
FoIA	folic acid
FR	folate receptor

## Abbreviations

---

G	Gauge (parameter for the diameter of hypodermic needles)
G1 phase	Gap 1 phase
h	hour(s)
HA	hyaluronic acid
i.v.	intravenous(ly)
i.t.	intratumoral(ly)
IVIS	<i>in vivo</i> imaging system
kg	kilogram(s)
KO	knockout
KRAS	Kirsten rat sarcoma virus
K-Ras protein	Kirsten rat sarcoma virus protein
mg, mm	milligram(s), millimeter(s)
miR	microRNA
miR-200(c)	microRNA 200(c)
miRISC	miRNA-containing RNA-induced silencing complex
miRNA	microRNA
mRNA	messenger RNA
MTX	methotrexate
n	number of samples
NaCl	sodium chloride
NTRK2	neurotrophic receptor tyrosine kinase 2
OAA	oligoaminoamide
p	p-value
PBS	phosphate buffered saline
PEG	polyethylene glycol

## Abbreviations

---

pH	potential of hydrogen
Ph.D.	Doctor of Philosophy
pre-miRNA	miRNA precursor
pri-miRNA	primary miRNA
RISC	RNA-induced silencing complex
RNA	ribonucleic acid
RNAi	RNA interference
RNase	ribonuclease
PCR	polymerase chain reaction
S phase	Synthesis phase
S.E.M.	standard error of the mean
siCtrl	small interfering control RNA
siRNA	small interfering RNA
SPAAC	strain-promoted alkyne-azide cycloaddition, click chemistry
Sph	succinoyl pentaethylene hexamine
SPPS	solid-phase assisted peptide synthesis
ss <sub>2</sub>	disulfide bond
Stp	succinoyl tetraethylene pentamine
TALEN	transcription activator-like effector nucleases
TfR	transferrin receptor
T <sub>H</sub> cell	T helper cell
TrkB	neurotrophic receptor tyrosine kinase 2, tyrosine receptor kinase B
WHO	World Health Organisation
XIAP	X-linked inhibitor of apoptosis
ZEB1/2	zinc finger E-box-binding homeobox 1/2



## I INTRODUCTION

In view of the numbers published by the WHO, the burden of fighting cancer displays an ascending role for the global society. With worldwide 19.3 million new cases and almost 10.0 million deaths in 2020, cancer remains not only a threat to public health but also ranks as one of the leading causes of death [1]. It is estimated that in 2040, 28.4 million new cancer cases are projected to arise [2].

Cancer emerges with the transformation of healthy cells into malignant tumor cells, which are characterized by abnormal and uncontrolled cellular growth [3]. The transformation is caused by genetic mutations that can be inherited as well as acquired through random or exposure-caused DNA replication errors [4, 5]. Causes for the latter type of DNA mutations comprise physical carcinogens including ultraviolet and ionizing radiation, chemical carcinogens like tobacco smoke components, and biological carcinogens covering certain viruses or bacteria [1, 6]. An accumulation of exposure to those risk factors in combination with less efficient cell repair mechanisms leads to a higher incidence with increased age [1].

Treating cancer is individually for every patient and specific for distinct cancer types. Hence, therapies often combine surgery, radiotherapy, and different types of chemotherapy [1]. The latter frequently goes along with chemoresistance, caused by various signaling pathways in cancer cells that lead to changes in gene expression and protein activity [7]. Also, surgery and radiotherapy show their limitations when the tumor is diffuse, inaccessible or when metastasis appears.

In consideration of the obstacles conventional therapy methods have to face, the need for new therapeutic approaches is incontestable. Hence, this thesis deals with an attempt to interfere in cancer cell growth via microRNA 200c

(miR-200c), a non-coding, endogenous RNA that covers approx. 20-22 nucleotides [8, 9].

## 1 The microRNA family

MicroRNAs (miRNAs) are essential components of the gene silencing machinery in most eukaryotic organisms [10]. By interfering with mRNA targets via pairing or by causing mRNA degradation, they are regulating protein expression at post-transcriptional level [11]. It is assumed that miRNAs regulate approx. 30% of mammalian protein-coding genes [12, 13], and that they give rise to several physiological processes like embryonic development, immune differentiation, metabolism, and cardiac function [11]. By contrast, miRNA imbalances can lead to diverse disorders like diabetes, cardiovascular disease, and cancer [14-16].

MiRNA biogenesis is a multistep process with subsections in the nucleus and the cytoplasm [17, 18]. Olejniczak *et al.* describe the biogenesis as follows: in the nucleus, RNA polymerase II transcribes miRNA genes into the several kilobases long primary miRNA (pri-miRNA). The further processing of the pri-miRNA is catalyzed by Drosha, a member of the ribonuclease III family (RNase III), and its RNA-binding cofactor DiGeorge syndrome critical region 8 (DGCR8). The Drosha-DGCR8 microprocessor complex cleaves the pri-miRNA near the base of its hairpin structure and finally releases the stem-loop structured miRNA precursor (pre-miRNA), containing approx. 70 nucleotides. In the next step, the pre-miRNA is shuttled by exportin-5 (EXP-5) from the nucleus into the cytoplasm. Further processing in the cytoplasm is carried out mainly by Dicer, a member of the RNase III family, and its cofactors, leading to the genesis of a double-stranded miRNA. After uncoiling the double-strand by the helicase activity of Dicer, the miRNA segregates into two single strands. The so-called passenger strand is rapidly degraded whereas the guide strand is packed into the RNA-induced silencing complex (RISC) [19]. The miRNA-

containing RNA-induced silencing complex (miRISC) exhibits an Argonaute (AGO) protein as a catalytic component [20, 21]. The AGO protein identifies the imperfectly complementary sequences in miRISC's target messenger RNA (mRNA) and, by uncapping and deadenylation, conveys its translational repression respectively transcript degradation [19, 22]. Hence, the effect of miRNA takes place at both the mRNA and the protein level [20]. **Figure 1** depicts the miRNA biogenesis process from the transcription of the miRNA gene to the formation of miRISC.

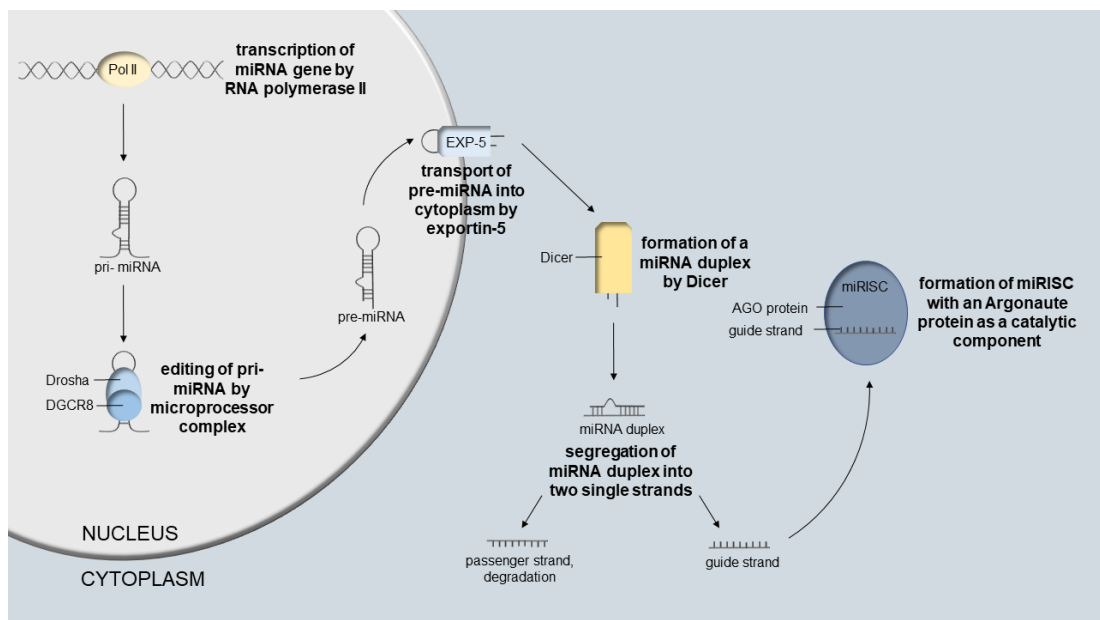


**Figure 1: miRNA biogenesis** from miRNA gene to miRISC formation.

### 1.1 MiRNAs in physiological and pathological processes

Complementary base pairing with various specific target mRNAs opens a wide field for miRNA actions in physiological and pathological processes. Whereas a normal miRNA expression provides proper development and homeostasis, dysregulation of miRNA levels may contribute to aberrant gene expression patterns leading to developmental disorders or dysfunctions in various fields [23].

For instance, a high expression of diverse miRNAs has been identified in all stages of cardiac development [24]. The relevance of miRNAs for a physiological heart function further has been approved by da Costa Martins *et al.*, who depleted the above-mentioned Dicer, which plays a key role in the miRNA biogenesis. The non-specific disruption of multiple miRNAs led to highly atrial enlargement and premature death in juvenile mice. In the adult myocardium, the loss of Dicer induced among other symptoms a severe biventricular enlargement, myocyte hypertrophy, and ventricular fibrosis [25]. MiRNAs also play a tremendous role in T cell differentiation and are therefore indispensable for a well-functioning immune system. Studies by Baumjohann *et al.* revealed that CD4<sup>+</sup> T cells with a lack of miRNA showed reduced survival and proliferation, meanwhile having enhanced sensitivity to signals that cause effector T helper cell (T<sub>H</sub> cell) differentiation and cytokine production. Additionally, several individual miRNAs and co-expressed miRNA clusters had been demonstrated to be decisive in T<sub>H</sub> cell fate and immune functions [20]. Furthermore, as stated by Andreeva *et al.*, miRNAs are essential in retinal development, preservation, and physiological function. Over 250 miRNAs are distinctively expressed in developing and adult mouse retina, present either ubiquitously or in a cell-specific form. Alterations in retinal miRNA expression or activity could be identified to be closely connected to frequent retinal disorders, such as age-related macular degeneration, diabetic retinopathy, retinitis pigmentosa, and retinoblastoma in human as well as in animal models [26].

Besides their contribution to a physiological heart, immune system and retinal function, various studies also state the significant role of miRNAs for other biological functions like brain development and neuroplasticity [27]; cholesterol, glucose, and fatty acid metabolism [28]; spermatogenesis, oogenesis and the development of the male and female reproductive tract [29].

## 1.2 MiR-200c and its influence on tumor cells

In line with their role in the above-mentioned biological processes, miRNAs are also closely involved in cancer formation. Thus, specific miRNA levels can be consistent with cancer type [30], stage, and other clinical variables [31]. For instance, Iorio *et al.* gave evidence that in human breast cancer a downregulation of miR-10b, miR-125b, and miR-145 occurred simultaneously with an upregulation of miR-21 and miR-155 [32]. In human glioblastoma, miR-221 was shown to be highly upregulated while miR-128, miR-181a, miR-181b, and miR-181c showed low levels [33].

In the context of cancer, there is a subgroup of miRNAs that is essential for cancer research and for comprehending the biological processes connected to the disease: The miR-200 family, consisting of miR-200a, miR-200b, miR-200c, miR-141, and miR-429 [34]. Processes like epithelial to mesenchymal transition (EMT), proliferation, cell invasion, metastasis, apoptosis, autophagy, and therapy resistance formation are widely affected by members of the miR-200 group [11].

Our working group has been focusing on a particular member of the miR-200 family during the last years: miR-200c and its effects on tumor cells have been evaluated in various studies whereby versatile knowledge in this field has been gained.

For instance, Kopp *et al.* demonstrated the significant role of miR-200c in avoiding acquired chemotherapy resistance in cancer cells. By treating BT474 breast cancer cells with the chemotherapeutic agent doxorubicin for several cycles, a chemoresistant phenotype was generated. A subsequent evaluation of miR-200c levels showed a significant down-regulation of miR-200c levels of BT474 cells with less susceptibility to doxorubicin. Additionally, inhibition of miR-200c in BT474 cells, usually a doxorubicin-sensitive cell line with a high miR-200c expression, showed to lead to significantly more resistant cells after

doxorubicin treatment. Reversely, in MDA-MB 436, a doxorubicin-resistant mesenchymal breast cancer cell line without miR-200c expression, induced overexpression of miR-200c triggered a higher sensitivity of the cells to doxorubicin [35]. The basis of this phenomenon could be identified as downregulation of two direct targets of miR-200c: neurotrophic receptor tyrosine kinase 2 (NTRK2 or TrkB), responsible for anoikis resistance in breast cancer [36] and B cell-specific Moloney murine leukemia virus integration site 1 (Bmi1), a regulator of stem cell self-renewal and senescence [35].

Further studies of our group revealed the connection between miR-200c and the proto-oncogene KRAS as KRAS was found to be directly targeted by miR-200c [37]. KRAS, as one of the most prominent oncogenes, is frequently mutated in many types of human tumors like pancreatic, colon, or lung cancer [38]. Findings by Kopp *et al.* stated that K-Ras protein expression was inversely correlating with the miR-200c expression level in a panel of different breast cancer cell lines like MDA-MB-436, MDA-MB-231, or BT474. Additional experiments with MDA-MB-231 cells, which bear an activating G13D mutation in the KRAS gene, and MDA-MB-436 cells, which express the wild-type KRAS gene, were performed: as K-Ras proteins are known to stimulate proliferation in various cell types, the proliferation of both cell lines was analyzed after pre-miR-200c or siRNA transfection. In the MDA-MB-231 cell line, the proliferation of pre-miR-200c- and siRNA treated cells was comparably hampered, while in MDA-MB-436 only pre-miR-200c significantly inhibited proliferation. Additionally, the cell cycle of MDA-MB-231 cells was notably changed through both pre-miR-200c and siRNA treatment, whereas only pre-miR-200c altered the cell cycle of MDA-MB-436 cells with a decreased G1 phase and an increased S phase for both cell lines as a result. In additional experiments, the same phenomenon could also be detected for the two non-small cell lung cancer cell lines A549 and Calu-1 [37].

As mentioned above, the influence of miR-200c on tumor cells is not only limited to its effects on chemoresistance and cell proliferation. It also plays a significant role in avoiding the epithelial-mesenchymal transition, EMT. Mutlu

*et al.* define EMT as the transformation of immotile epithelial cells to motile and invasive mesenchymal cells by losing their cell-to-cell adhesion properties [8, 9]. Therefore, EMT is a decisive step in the metastatic cascade and contributes pathologically to cancer progression [9, 39]. A characteristic phenomenon of EMT is the increase of levels of mesenchymal proteins, accompanied by the functional loss of the cell surface marker E-cadherin [40, 41]. Transcription factors, primarily ZEB1 and ZEB2, repress the E-cadherin expression [40, 41] and therefore trigger the EMT and consequently initiate early steps of metastasis [9]. MiR-200c and other members of the miR-200 family directly target the E-cadherin repressors ZEB1 and ZEB2, thus determine the epithelial phenotype of cancer cells and inhibit EMT [42]. This phenomenon was emphasized by Mueller *et al.* of our working group through efficient delivery of miR-200c via our maleimide-PEG-GE11 **454** polyplexes that led to a significant downregulation of ZEB1 expression in MDA-MB-231 breast cancer cells as well as in T24 bladder carcinoma. In addition to the effects on EMT via targeting ZEB1, significantly inhibited cell proliferation, improved susceptibility of these cells to doxorubicin, and a change of the cell cycle with a significantly increased number of cells in the S phase could be observed. Further, for MDA-MB-231 cells, an inhibition of tumor cell migration was detected [43].

To outline further possible underlying causes of miR-200c effects, our working group performed a proteomic analysis of an *in vitro* knockout of miR-200c. Therefore, a TALENs (transcription activator-like effector nucleases) knockout of miR-200c in MCF7 breast cancer cells was created, while its compensation by other members of the miR-200 family was excluded [11]. TALENs are DNA-binding proteins connected to a non-specific endonuclease domain causing DNA double-strand breaks [44]. Thus, a disruption of the miR-200c gene by mutations through error-prone non-homologous end-joining was caused [11]. Ljepoja *et al.* identified 26 key proteins to be either upregulated or downregulated by a miR-200c knockout. A majority of these proteins (for example Filamin A/B (FLNA/FLNB), Tropomyosin alpha-1 chain) are attributed to the regulation of cell migration, others like Aspartate aminotransferase or 4F2 cell-surface antigen heavy chain regulate cell metabolism, respectively

apoptosis. In addition, proteins with detoxification or unknown function could be identified. All in all, alterations in protein expression went along with additionally observed biological phenomena like increased migration and chemoresistance as well as altered metabolism that were found in the miR-200c-KO clones [11].

### 1.3 Inducible miR-200c in breast cancer cells

To further evaluate the reported emerging effects of a miR-200c-KO, our working group has previously designed miR-200c inducible MDA-MB-231 and MCF7 cell lines. Ljepoja *et al.* transduced MDA-MB-231 cells, which lack miR-200c expression, and the above-mentioned miR-200c knockout MCF7 cells with a doxycycline-inducible miR-200c expression construct (TRIPZ-200c) or an inducible scrambled control (TRIPZ-Ctrl) utilizing a lentiviral carrier system.

Afterward, by doxycycline induction of miR-200c expression, motility of TRIPZ-200c treated and TRIPZ-Ctrl treated cells was compared. A multi-parameter analysis of motility revealed that the induced miR-200c expression in MDA-MB-231-TRIPZ-200c cells resulted in reduced motility of cells and an overall decreased migratory potential [45]. As MDA-MB-231 cells are not or only weakly expressing E-cadherin [46, 47], observed phenomena were suspected to be independent of the ZEB1/2-induced EMT mechanisms. Interestingly, FLNA, a regulator of cell migration that was detected by our group to be upregulated after a miR-200c knockout in MCF7 cells, was observed to be downregulated in the MDA-MB-231-TRIPZ-200c cells after doxycycline-induced miR-200c expression. Further, an investigation of cellular morphology showed that while the TRIPZ-Ctrl cells sustained their mesenchymal, spindle-like shape, the miR-200c expression modified the cellular phenotype towards rounder, consistently dilated, and flatter cells [45].

To further investigate those promising findings of our working group *in vivo*, for this thesis we inoculated miR-200c-inducible MDA-MB-231-TRIPZ-200c-CMV-Luc cells as well as non-inducible MDA-MB-231-TRIPZ-Ctrl-CMV-Luc cells, both containing an additional luciferase gene, as tumor xenograft models into mice. As the constant luciferase expression of cells leads to a luminescent signal after contact with luciferin, tumors could be observed not only macroscopically but also by *in vivo* luminescence imaging. Via feeding mice either with doxycycline-containing or doxycycline-free feed, effects of induced miR-200c on tumor formation and tumor growth could be evaluated.

#### 1.4 Therapeutic use of miRNAs

With the current level of knowledge, an intervention into the miR-200c level precisely or deregulation of miRNA expression in general seem to be promising approaches to develop efficient new RNA interference (RNAi) therapeutics.

For RNAi therapeutics in the field of miRNAs, two types of therapeutic reagents are in the focus of current research: miRNA mimics and antagomiRs. AntagomiRs suppress the function of specific miRNAs that may be overexpressed in a certain disease [48]. Inversely, miRNA mimics try to re-achieve physiological levels of a specific miRNA that is suppressed with the occurrence of a certain pathology [49]. As this thesis deals with an attempt to deliver a miR-200c mimic via sequence-defined oligoaminoamides into breast cancer cells, the focus of the paragraph below lies on the intracellular delivery of miRNA mimics.

#### 1.4.1 Obstacles of miRNA delivery

To obtain sufficient circulation time, miRNA-based therapeutics must overcome obstacles such as their degradation by nucleases [50] or by the immune system as well as being eliminated through renal clearance [51]. Furthermore, the delivery into the tumor cell is challenged by crossing the endothelium and by effective endocytosis and endosomal release mechanisms; third, unintentional side effects through an immune response or toxicity reactions have to be prevented or limited [51]. For improved biosafety, it is also essential to avoid accumulation in the body, to minimize uncontrolled off-targeting due to 'chemical stickiness', and to pass the physical/biological barriers in a controlled process [52].

#### 1.4.2 Sequence-defined oligoaminoamides

To overcome those hurdles, the use of carrier systems with definite characteristics is inevitable. Two major groups of carriers can be distinguished: Viral and non-viral vectors. Viral vectors show, due to the potential of viruses to efficiently infect host cells, high efficacy in transfection [53]. Nevertheless, certain disadvantages like a limited packing capacity, virus immunogenicity, and a complex, expensive, and time-consuming synthesis remain [54]. Non-viral vectors like cationic polymers and liposomes [55] bypass certain of those disadvantages. Together with anionic nucleic acids like miRNAs they can form stable nanoparticles, the so-called lipo- or polyplexes [56].

Our group aims at developing new, effective cationic carrier systems. To this day, our library comprises over 1500 sequence-defined oligoaminoamides (OAAs), so-called oligomers. These small polycations are processed in a sequence-defined manner via solid-phase assisted peptide synthesis (SPSS) [57]. SPSS opens the possibility to easily alter functional moieties and their position within such artificial peptide-like structures via modular design.

Functional units of interest are, inter alia, structural motifs for nucleic acid binding, endosomal escape, nanoparticle stabilization, and carrier biodegradability [58].

In general, an oligomer consists of a linear backbone, containing building blocks like the artificial amino acids succinoyl pentaethylene hexamine (Sph) or succinoyl tetraethylene pentamine (Stp). Due to their cationizable aminoethylene motif, both can bind nucleic acids and are therefore decisive components for polyplex formation [59]. Further, together with additionally integrated histidines, they can enhance endosomal escape by providing an endosomal buffering effect [60]. Other polyplex-stabilizing constituents are disulfide bond-forming cysteines [61] or tyrosine tripeptides [62] and fatty acids (forming lipo-OAAs) [63].

OAAs can be subdivided into topological subclasses like linear, 2-arm, 3-arm, 4-arm, or T-shaped oligomers. The described polymer **1214** (illustrated in **Figure 2**) exhibits a T-shaped form. Its cationic Stp-backbone enables polyplex formation when combined with a negatively charged nucleic acid [59]. For stability reasons, tyrosines and cysteines were added, whereas histidines should facilitate the endosomal escape of **1214**. To enable post-functionalization via strain-promoted alkyne-azide cycloaddition (SPAAC, “click chemistry”) with dibenzocyclooctyne (DBCO) click agents like hyaluronic acid (HA), azido-lysines were incorporated [64, 65]. In case of **1214**, two oleic acid units, fixed at the cationic backbone, form the hydrophobic domain. The function of oleic acid consists of providing improved stability; further, the hydrophobic group facilitates the escape of polyplexes from endosomes to the cytosol for its endosomal, pH-dependent lytic activity [57].

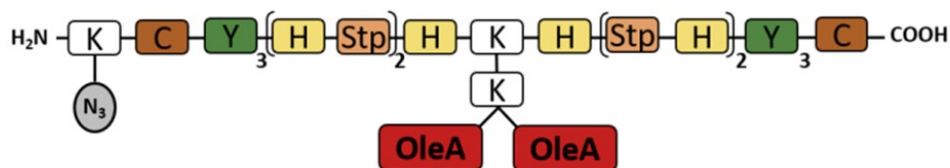


**Figure 2: Simplified depiction of T-shaped oligomer 1214.** Elements of **1214** are: K: lysine C: cysteine, Y: tyrosine, H: histidine, Stp: succinoyl tetraethylene pentamine, N<sub>3</sub>: azide function, and OleA as oleic acid. Figure provided by Dr. Jie Luo, former Ph.D. student at the Faculty for Chemistry and Pharmacy, Ludwig Maximilian University, Munich.

### 1.4.3 Shielding components

When therapeutic polyplexes get into contact with blood components, the formation of a so-called “protein corona” is likely to happen. In the bloodstream, a layer of biomolecules, predominantly proteins, enshroud the nanoparticles and thus mediate their subsequent behavior [66, 67]. Not only cellular uptake, but also immune response, biodistribution, clearance, and toxicity can be changed [68]. To circumvent those unwanted alterations, particle shielding is essential for polyplex formation. An effective shielding is not only reducing the protein corona but also prolonging circulation time, leading to improved passive targeting by the enhanced permeability and retention (EPR) effect [69].

A common candidate as a shielding agent is polyethylene glycol (PEG) [70]. PEGylation, coating the surface of nanoparticles with the hydrophilic PEG reduces the formation of a protein corona [71] and improves the colloidal and biological characteristics [72] like biocompatibility, hydrophilicity, stability, and biodegradability [73]. Nevertheless, recent studies demonstrate the occurrence of anti-PEG immunity [74-76]. Antibodies that specifically bind PEG can lead to the “accelerated blood clearance” of PEGylated therapeutics [77] and to an increase in adverse effects [78]. Approx. 20% of healthy humans

show pre-exposure anti-PEG antibodies prior to treatment with PEGylated therapeutics [79].

An alternative shielding agent is, among others, hyaluronic acid (HA), an anionic polysaccharide and component of the extracellular matrix and synovial fluids [80]. HA, for its negative charge, veils the positive charge of the polyplex and therefore can be suspected to reduce nonspecific interactions between anionic blood components and the polyplex. Thus, decreased toxicity, improved *in vivo* stability, and enhanced therapeutic effects and biodegradability can be expected [81, 82].

#### 1.4.4 Targeting components

As mentioned above, shielding components improve the transfection effect through passive parameters like preventing the polyplex from interacting with blood components and leading to an EPR effect. In contrast to shielding agents, active targeting compounds aim to convey the active entry into the tumor cell with subsequent liberation of the nucleic acid into the cytoplasm. Hence, ligands or antibodies, which actively target selected tumor cells enhance the specificity of the therapeutic nanoparticle [83, 84]. As a consequence, the increased affinity to tumor cells in comparison to healthy cells through active targeting leads to a maximized efficacy accompanied by enhanced safety of the therapeutic agent [85].

As many tumor cells overexpress multiple specific receptors [86-88], a wide range of possible targets for suitable active ligands appears. For instance, the folate receptor (FR) is overexpressed in various solid tumor cells like ovarian, kidney, brain, or lung cancer [89, 90]. Through their high affinity and high specificity coupled with the ability of folate-receptor-mediated endocytosis, chemotherapeutic folate targeting is a frequently used method in cancer therapy [91]. Further possible targets are e.g. the transferrin receptor (TfR),

overexpressed in a majority of malignant cells e.g. in cancer types like chronic lymphocytic leukemia [92]; or the epidermal growth factor receptor (EGFR), generally overexpressed in several malignancies related to angiogenesis, proliferation, invasion, and metastasis of the tumor cells [93]. Additionally, the aforementioned hyaluronic acid can not only serve as a shielding agent but also targets CD44 [94, 95], a cell-surface glycoprotein and a common marker of cancer stem cells in breast cancer [96], but also expressed in other cancer cells like in cervical cancer [97].

Our working group has been evaluating various target receptors in multiple experiments. Truebenbach *et al.* synthesized a set of folic acid (FolA)- and methotrexate (MTX)-oligoamides and investigated, inter alia, their effect on the viability of FR-overexpressing human carcinoma KB and murine leukemia L1210 cells [98]. Other experiments successfully demonstrate the high efficacy of FolA-targeting *in vivo* [99]. Referring to TfR-targeting, we could significantly increase gene transfer activities in the TfR overexpressing cell lines K562, DU145, and KB with a series of polyplexes containing transferrin-conjugates [100]. Furthermore, polyplexes modified with EGFR targeting peptide GE11 facilitated silencing of an enhanced green fluorescent protein (EGFP)-luciferase reporter gene in EGFR overexpressing KB and Huh7 cells [101]. Additionally, as mentioned above, our GE11-targeted **454** miR-200c polyplexes led to a significant downregulation of ZEB1 expression in MDA-MB-231 breast cancer cells as well as in T24 bladder carcinoma [43].

In this thesis, a sub-experiment deals with the delivery of miR-200c into MDA-MB-231 breast cancer cells of tumor-bearing mice. As the MDA-MB-231 cell line is expressing CD44 [102, 103], we used HA as a passive and active targeting ligand. Dibenzocyclooctyne (DBCO)-amine-modified HA was functionalized with the miR-200c-containing **1214** via copper-free click reaction and injected intratumorally. Due to its similar structure and biological function to miRNA-200c, we decided to use siRNA as a control nucleic acid [104]. Therefore, also siCtrl was modified with **1214** and functionalized with DBCO-amine-modified HA.

## 2 Aims of the thesis

Through various *in vitro* studies, our working group has been proposing the outstanding effect of miR-200c on preventing EMT, metastasis, and chemoresistance in breast cancer. This thesis aimed at exploring the effects of miR200c in a murine xenograft model of human breast cancer *in vivo*.

In this regard, an alteration of miR-200c levels in subcutaneous MDA-MB-231-TRIPZ-200c-CMV-Luc tumors was obtained via doxycycline-induced increased transcription of the miR-200c gene, and tumor development had to be evaluated. Furthermore, we evaluated intratumoral delivery of miR-200c-nanoparticles formulated with hyaluronic acid as shielding and targeting ligand as a therapeutic approach for the development of future RNAi therapeutics.

In the next step, the effect of transcriptionally induced miR-200c in MDA-MB-231-TRIPZ-200c-CMV-Luc tumors on efficacy of chemotherapy with doxorubicin had to be evaluated.

Additionally, as control experiments, we intended to exclude an influence of doxycycline itself on tumor growth in order to verify miR-200c as the origin of all effects on tumor development in case of the doxycycline-induced miR-200c levels.



## II MICE, MATERIALS AND METHODS

### 1 Mice

#### 1.1 Mouse strain

5-week-old Female Rj: NMRI-Foxn1<sup>nu</sup>/Foxn1<sup>nu</sup> mice were purchased from Janvier Labs (Le Genest-Saint-Isle, France). The outbred strain shows a mutation in the Foxn1 gene that leads to thymic aplasia. Consequently, mice do not exhibit mature T-cells, whereas B-lymphocytes and all components of the innate immune system remain functional. As the mutation also causes a keratinization defect of the hair follicle and epidermis, mice are nude [105]. Due to their immunodeficiency in terms of T-lymphocytes, NMRI-Foxn1<sup>nu</sup>/Foxn1<sup>nu</sup> mice are a suitable model for xenograft tumor experiments. Further, their lack of fur makes them an ideal model for bioimaging experiments.

#### 1.2 Housing conditions

After arrival at our animal facility, mice passed an acclimatization time of at least one week. Mice were kept in isolated ventilated cages (IVC type II, Tecniplast, Hohenpeißenberg, Germany) under specific pathogen-free conditions, which were monitored quarterly by a health analysis of two sentinel animals. A 12 h day/night interval was maintained. Temperature and air humidity were recorded daily and kept between 23 °C and 26 °C respectively 50% and 70%. Light intensities did not exceed 200 Lux, sound intensities kept under 40 dB. The stocking density of each cage varied between 2 and 5 mice. Dust-free bedding (ABEDD Vertriebs GmbH, Vienna, Austria) was provided and, together with water and feed, changed weekly. Feed was obtained from ssniff Spezialdiäten (Soest, Germany) and both, feed and water were offered

*ad libitum*. Cottages, wooden tubes, and nesting material were allocated. Housing and nourishment components were sterilized by autoclaving before getting into contact with mice. Animal welfare was controlled and protocolled daily and in accordance with the official permission based on §11 of the German Animal Welfare Act [106].

### 1.3 Health monitoring

Sentinel mice were kept at the same location and under the same conditions as experimental animals. Once weekly, sentinel cages were prepared with used bedding material and feed of the cages of experimental animals. Every three months, a complete health analysis of two sentinel mice was performed by an external laboratory (mfd Diagnostics GmbH, Wendelsheim, Germany). No findings were identified for all experimental animals in this project.

## 2 Materials

### 2.1 Cell culture

Material	Source
MDA-MB-231-Tripz-200c-CMV-Luc cells (human breast cancer cells)	Faculty for Chemistry and Pharmacy, Ludwig Maximilian University (Munich, Germany)
MDA-MB-231-Tripz-Ctrl-CMV-Luc cells (human breast cancer cells)	Faculty for Chemistry and Pharmacy, Ludwig Maximilian University (Munich, Germany)
Leibovitz's L-15 medium	Thermo Fischer Scientific (Waltham, USA)

FCS	Invitrogen (Karlsruhe, Germany)
PBS	Biochrom (Berlin, Germany)
Cell culture plates and flasks	TPP (Trasadingen, Switzerland)

## 2.2 Polyplexes

The oligomer **1214** (illustrated in **Figure 2**) was synthesized by Simone Berger and Victoria Vetter, both Ph.D. students at the Faculty for Chemistry and Pharmacy, Ludwig Maximilian University, Munich.

## 2.3 Nucleic acids and compounds

Material	Source
MiR-200c	Axolabs (Kulmbach, Germany)
SiCtrl	Axolabs (Kulmbach, Germany)
Hyaluronic acid	Lifecore Biomedical (Chaska, USA)
Doxorubicin hydrochloride	Sigma-Aldrich (Taufkirchen, Germany)
Luciferin	Sigma-Aldrich (Taufkirchen, Germany)

## 2.4 Animal treatment equipment

Material	Source
Isoflurane CP®	CP-Pharma (Burgdorf, Germany)
Bepanthen®	Bayer Vital GmbH (Leverkusen, Germany)
Syringes, needles	BD Medical (Heidelberg, Germany)

## 2.5 Doxycycline feed

625 mg/kg doxycycline-containing, estrogen-free, irradiated feed was obtained from ssniff Spezialdiäten (Soest, Germany).

## 2.6 Instruments

Instrument	Source
Caliper DIGI-Met	Preisser (Gammertingen, Germany)
IVIS Lumina	Caliper Life Sciences GmbH (Hopkinton, USA)

## 2.7 Software

Software	Source
GraphPad Prism 9	GraphPad Software (San Diego, USA)
Living Image 3.2	Caliper Life Sciences GmbH (Hopkinton, USA)

## 3 Methods

### 3.1 Cell culture

MDA-MB-231-Tripz-200c-CMV-Luc cells and MDA-MB-231-Tripz-Ctrl-CMV-Luc cells were cultured in Leibovitz's L-15 medium supplemented with 10% fetal calf serum (FCS). The cell lines were cultured at 37 °C and 0% CO<sub>2</sub> in an incubator. Cells were cultured and provided by Bianca Köhler, Ph.D. student at the Faculty for Chemistry and Pharmacy, Ludwig Maximilian University, Munich.

### 3.2 *In vivo* experiments

For xenograft tumor experiments, tumor cells were suspended in 150 µl PBS and injected into the left flanks of 6 to 7-week-old NMRI-Foxn1<sup>nu</sup>/Foxn1<sup>nu</sup> mice with a syringe and a 27G cannula. The inoculation was performed under inhalation anesthesia (4% isoflurane in oxygen for induction, 2.5% for maintenance). The health status and well-being of mice as well as their weights were monitored daily. Tumor sizes were determined by caliper and volumes were calculated with the common formula [0.5 x longest diameter x shortest

diameter<sup>2</sup>] [107]. Intratumoral injections were performed under short isoflurane anesthesia and limited to a maximum of 7 injections with a minimum 2-day rest in between for reasons of animal welfare. Intravenous injections were performed by fixing mice in a restrainer and injecting a maximum volume of 150  $\mu$ l into their lateral tail vein. Intravenous injections were limited to a maximum of 4 injections with a minimum 6-day rest in between. All mice were sacrificed when pre-defined termination criteria were reached or as soon as tumor diameter extended a size of 12 mm. Animals were also euthanized if their well-being was severely affected through e.g. automutilation, constant weight loss, or continual signs of pain. Euthanasia was performed by cervical dislocation under isoflurane anesthesia.

All animal experiments were approved by the district government of Upper Bavaria (reference number: 55.2-2532.Vet\_02-19-20) and were consistent with the guidelines of the German Animal Welfare Act [106].

### 3.2.1 Effect of miR-200c on tumor formation and growth

At their arrival, 5-week-old NMRI-Foxn1<sup>nu</sup>/Foxn1<sup>nu</sup> mice were randomly divided into 2 groups of 20 animals each, receiving permanently either 625 mg/kg doxycycline-containing feed or control feed without doxycycline. After 7 days, mice were injected subcutaneously with  $5 \times 10^6$  MDA-MB-231-Tripz-200c-CMV-Luc cells as described above. Tumors were observed daily and, as soon as they were measurable, measured by caliper. When tumors reached sizes of approx. 200 mm<sup>3</sup>, the experiment was terminated, and animals were further subdivided into treatment groups of chapter 3.2.4.

### 3.2.2 Influence of doxycycline on tumor growth

At their arrival, 5-week-old NMRI-Foxn1<sup>nu</sup>/Foxn1<sup>nu</sup> were randomly divided into 2 groups of 10 animals each, receiving permanently 625 mg/kg doxycycline-containing feed, respectively control feed without doxycycline. After 7 days, mice were injected subcutaneously with  $5 \times 10^6$  MDA-MB-231-Tripz-Ctrl-CMV-Luc cells. Tumors were observed daily and, as soon as they were measurable, measured by caliper. As the MDA-MB-231-Tripz-Ctrl-CMV-Luc cell line tends to develop necrosis, only animals with a normal tumor growing behavior were taken up into the experiment. Mice that showed tumor necrosis were sacrificed. The pre-defined termination of the experiment and euthanasia of animals were set as the date when tumors reached a size of approx. 700 mm<sup>3</sup>.

### 3.2.3 Intratumoral application of polyplexes

$5 \times 10^6$  MDA-MB-231-Tripz-200c-CMV-Luc cells were inoculated subcutaneously into 6-week-old NMRI-Foxn1<sup>nu</sup>/Foxn1<sup>nu</sup> mice. On day 23 after tumor inoculation, when tumors were slightly visible with a volume between 30 mm<sup>3</sup> and 50 mm<sup>3</sup>, mice were randomized and divided into 2 groups of 10 animals. Both groups were intratumorally injected with 50  $\mu$ l of **1214** (containing 40  $\mu$ g of miR-200c, respectively 40  $\mu$ g of siCtrl) with 0.1 equiv. of DBCO-amine-modified HA. 6 further intratumoral injections were performed on days 27, 30, 34, 37, 41, and 44 after tumor inoculation. Tumors were observed/measured by caliper daily. The pre-defined termination of the experiment and euthanasia of animals were set as the date when tumors exceeded a diameter of 12 mm<sup>3</sup>, analogical to a tumor size of around 850 mm<sup>3</sup>. Tumor-free animals were euthanized on day 150 after tumor inoculation.

### 3.2.4 Antitumoral effects of miR-200c and doxorubicin

The evaluation of possible effects of miR-200c on the susceptibility of tumor cells to the chemotherapeutic agent doxorubicin contains 2 separate experiments.

#### (a) Sub-experiment a)

The first experiment was performed with mice of 3.2.1: 'Effect of miR-200c on tumor formation and growth' as soon as their tumors had reached sizes of approx. 200 mm<sup>3</sup>. As mentioned in 3.2.1., since their arrival, mice had permanently been receiving 625 mg/kg doxycycline-containing feed or control feed without doxycycline. At a tumor volume of approx. 200 mm<sup>3</sup>, every mouse was individually sub-divided into 1 of 4 groups and equivalently treated as follows: Mice that had been receiving doxycycline-containing feed additionally obtained either intravenous chemotherapy with 5 mg/kg doxorubicin (in a total volume of 150 µl) or intravenous control treatment with 150 µl NaCl. Control-fed mice also received either chemotherapy or control treatment as indicated. Mice were injected every 7 days, 4 times in total. The pre-defined termination of the experiment and euthanasia of animals were set as the date when tumors exceeded a diameter of 12 mm<sup>3</sup>, analogical to a tumor size of around 850 mm<sup>3</sup>. **Figure 3** gives an overview of all treatment groups of experiment 3.2.4 a).

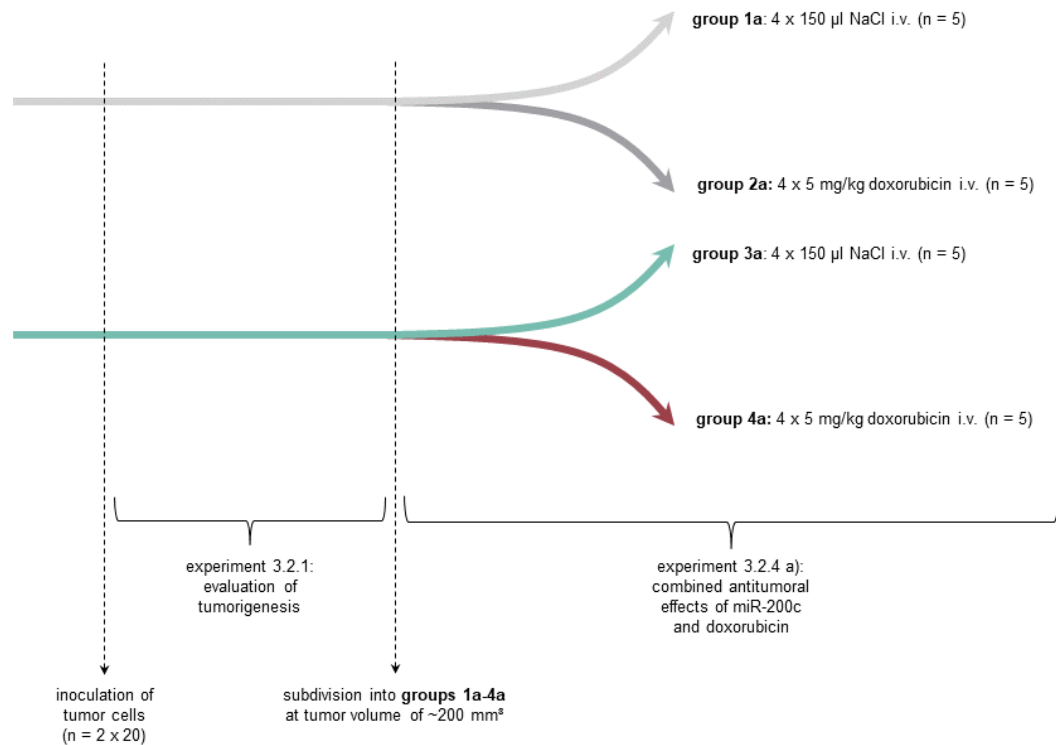


**Figure 3: Experimental settings of 3.2.4 a).** Grey arrows represent animals receiving control feed, blue/red arrows represent animals receiving feed containing 625 mg/kg doxycycline.

(b) Sub-experiment b)

The second experiment was performed independently from the first part. 40 NMRI-Foxn1<sup>nu</sup>/Foxn1<sup>nu</sup> mice were subcutaneously injected with  $5 \times 10^6$  MDA-MB-231-Tripz-200c-CMV-Luc cells. Tumors were observed daily and, as soon as they were measurable, measured by caliper. At a size of 130 mm<sup>3</sup> to 150 mm<sup>3</sup>, mice were individually divided into 4 groups of 10 animals each. Group 1 kept the normal control diet and got intravenously injected with NaCl, whereas group 2 obtained the control diet additionally to an intravenous chemotherapy of 5 mg/kg doxorubicin. Group 3 was fed with 625 mg/kg doxycycline-containing feed and received an intravenous NaCl control treatment. Group 4 also got its feed switched into doxycycline-containing feed and received intravenous chemotherapy of 5 mg/kg doxorubicin.

All intravenous injections contained a maximum volume of 150  $\mu\text{l}$  and were performed every 7 days, 4 times in total. Due to their premature euthanasia because their tumor sizes exceeded the pre-defined limit, 3 animals of group 1 received only 3 injections. The pre-defined termination of the experiment and euthanasia of animals were set as the date when tumors exceeded a diameter of 12  $\text{mm}^3$ , analogical to a tumor size of around 850  $\text{mm}^3$ . **Figure 4** constitutes all treatment groups of experiment 3.2.4 b).

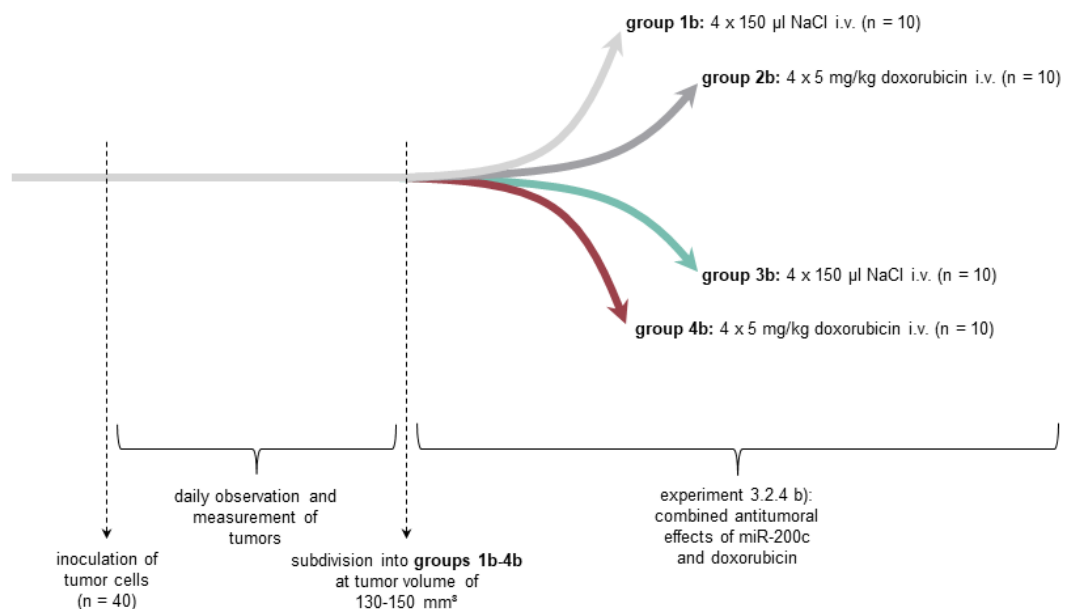


**Figure 4: Experimental settings of 3.2.4 b).** Grey arrows represent animals receiving control feed, blue/red arrows represent animals receiving feed containing 625 mg/kg doxycycline.

### 3.2.5 Bioimaging as validation of tumor absence

Mice with non-visible tumors of sub-experiment 3.2.4 b) were imaged for luminescence as soon as tumors were not macroscopically visible anymore. Under isoflurane anesthesia (4% isoflurane in oxygen for induction, 2.5% for maintenance), mice received an intraperitoneal injection of 100 mg/kg luciferin in 150  $\mu$ l PBS. For the intraperitoneal injection, a 30G cannula was used. 5 minutes after luciferin injection, imaging was conducted under the aforementioned anesthesia in the IVIS Lumina device. Mice were imaged a second time between days 120-140 after the first treatment. For the image evaluation, luminescence signals were analyzed using the software Living Image 3.2.

### 3.3 Statistical analysis

Results are expressed as mean + S.E.M. unless indicated otherwise. Statistical analysis was performed with one-way analysis of variance, unpaired students t-test or log-rank test using the software GraphPad Prism 9. P-values < 0.05 were determined as significant (\*p < 0.05; \*\*p < 0.01; \*\*\*p < 0.001; \*\*\*\*p < 0.0001; ns = not significant).



### III RESULTS

This chapter comprises an *in vivo* evaluation of the effects of an intervention in miR-200c levels of MDA-MB-231-Tripz-200c-CMV-Luc breast cancer cells on tumor growth and chemotherapy in a murine xenograft model (NMRI-Foxn1<sup>nu</sup>/Foxn1<sup>nu</sup>). Therefore, the alteration of miR-200c levels was obtained on the one hand by doxycycline-induced increased transcription of the miR-200c gene. Secondly, a modification of intracellular miR-200c amount was aimed via intratumoral delivery of **1214** miR-200c-nanoparticles formulated with HA-DBCO as shielding and targeting ligand.

The influence of doxycycline itself on tumor growth was appraised with MDA-MB-231-Tripz-Ctrl-CMV-Luc breast cancer cells under pre- and absence of doxycycline in NMRI-Foxn1<sup>nu</sup>/Foxn1<sup>nu</sup> mice.

HA-modified **1214** miR-200c nanoparticles were generated by Simone Berger and Victoria Vetter, both Ph.D. students at the Faculty for Chemistry and Pharmacy, Ludwig Maximilian University, Munich. Ulrich Wilk and Jana Pöhmerer, also Ph.D. students at the Faculty for Chemistry and Pharmacy, Ludwig Maximilian University, Munich, assisted during *in vivo* studies.

#### 1 Effect of miR-200c on tumor formation and growth

To evaluate the effect of induced miR-200c on tumor formation and early tumor growth, 40 NMRI-Foxn1<sup>nu</sup>/Foxn1<sup>nu</sup> mice were randomly divided into 2 groups of 20 animals each, receiving permanently either doxycycline-containing feed to induce endogenous miR-200c expression or control feed without doxycycline. After seven days, the inoculation of MDA-MB-231-Tripz-200c-CMV-Luc cells was performed, and tumorigenesis was observed respectively measured from that day on.

**Figure 5** shows the tumor growth of both groups from the day of tumor inoculation until, due to their tumor size of approximately 200 mm<sup>3</sup>, the first animals of the respective groups were further sub-divided for a follow-up experiment. The doxycycline group with endogenous miR-200c expression revealed a significant tumor growth inhibition: on day 33, the control group exceeded a volume of 100 mm<sup>3</sup> whereas the doxycycline group still showed almost no tumor growth. Further, on day 90, the mean volume of the doxycycline group amounted below 40 mm<sup>3</sup>, which was still under the 100 mm<sup>3</sup> of the control group on day 33. In **Figure 6**, the share of visible tumors after tumor cell inoculation is represented until the first animals of the respective groups were euthanized. Also here, a significant difference is detectable. On day 22, 100% of control mice had been developing tumors, whereas only 5% of doxycycline-fed mice showed a visible tumor that day. Further, until day 106, only 50% of the miR-200c expressing mice exhibited a visible tumor, and 8 out of 19 animals did not develop a tumor at all until the day of sacrifice.

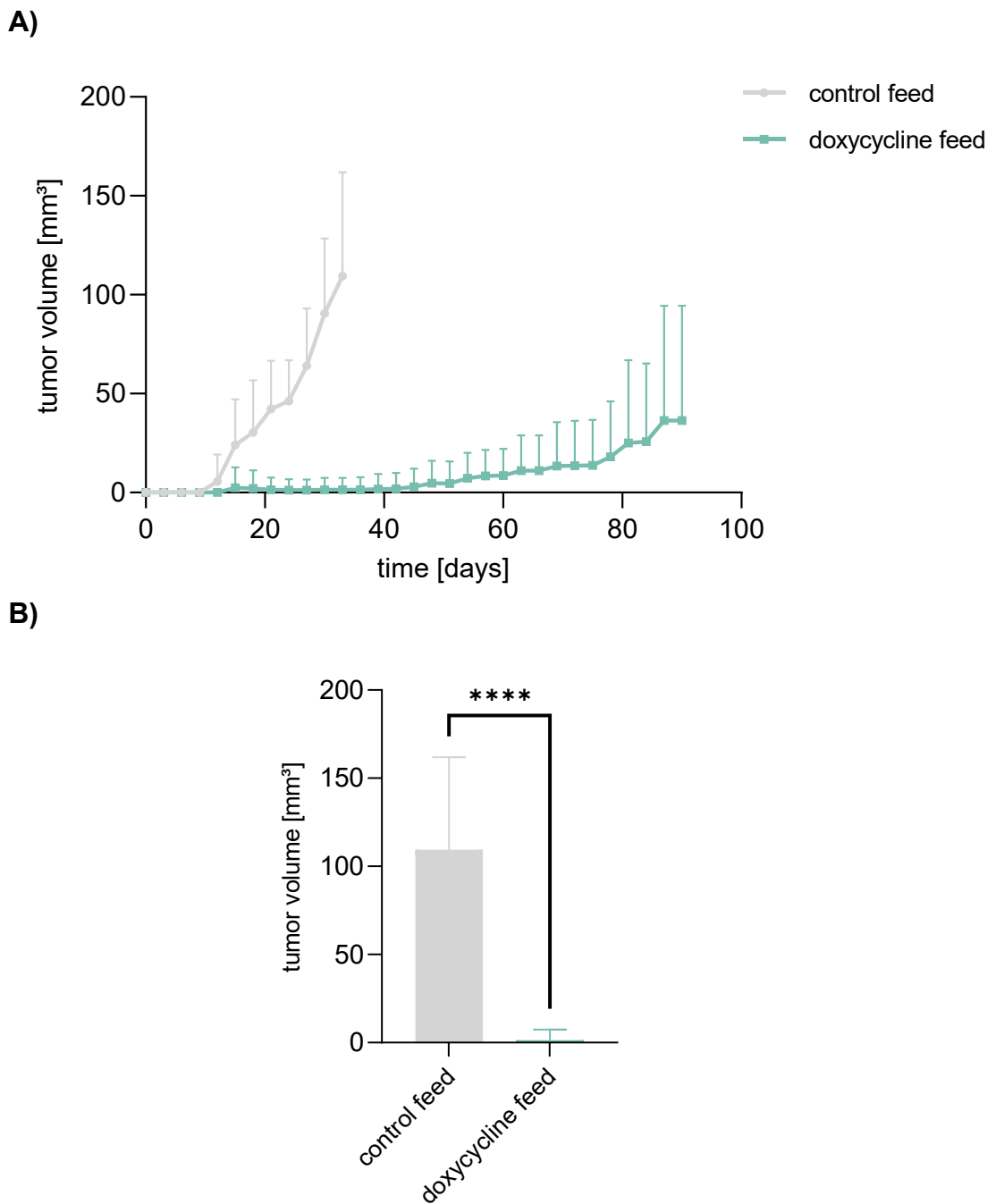


**Figure 5: Tumor growth** of MDA-MB-231-Tripz-200c-CMV-Luc tumor-bearing mice, fed with doxycycline-containing feed for miR-200c induction, respectively control feed. **A)** Tumor growth of groups throughout the experiment. Day 0 represents the day of tumor cell inoculation. Data shown until the first animals of the respective groups were subdivided into groups for further experiments (mean + S.E.M.; n = 20/19 (control feed/doxycycline feed)). **B)** Comparison of tumor sizes on day 33 after tumor cell inoculation (mean + S.E.M.; n = 20/19 (control feed/doxycycline feed); \*\*\*\*p < 0.0001).

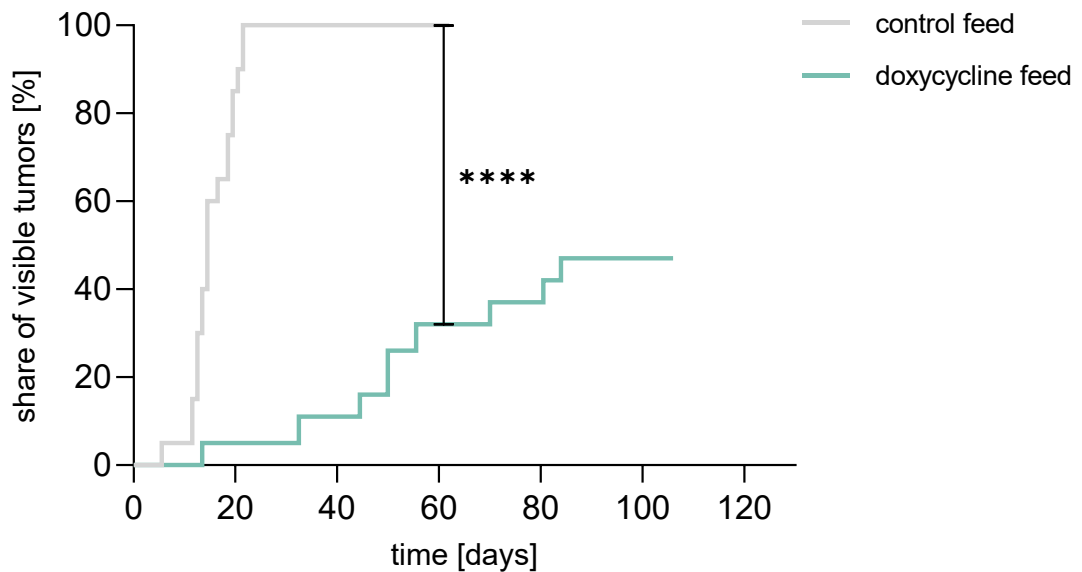


**Figure 6: Share of visible tumors** of MDA-MB-231-Tripz-200c-CMV-Luc tumor-bearing mice, fed with doxycycline-containing feed for miR-200c induction, respectively control feed. Day 0 represents the day of tumor cell inoculation. Data shown until the first animals of the respective groups were euthanized (mean + S.E.M.; n = 20 / 19 (control feed / doxycycline feed); \*\*\*\*p < 0.0001).

To ensure the uptake of doxycycline feed and its tolerability, mice were weighed daily. The similar weight development of both groups, which is displayed in **Figure 7**, suggests that doxycycline feed and the resulting miR-200c expression in tumor cells were well tolerated by the animals.

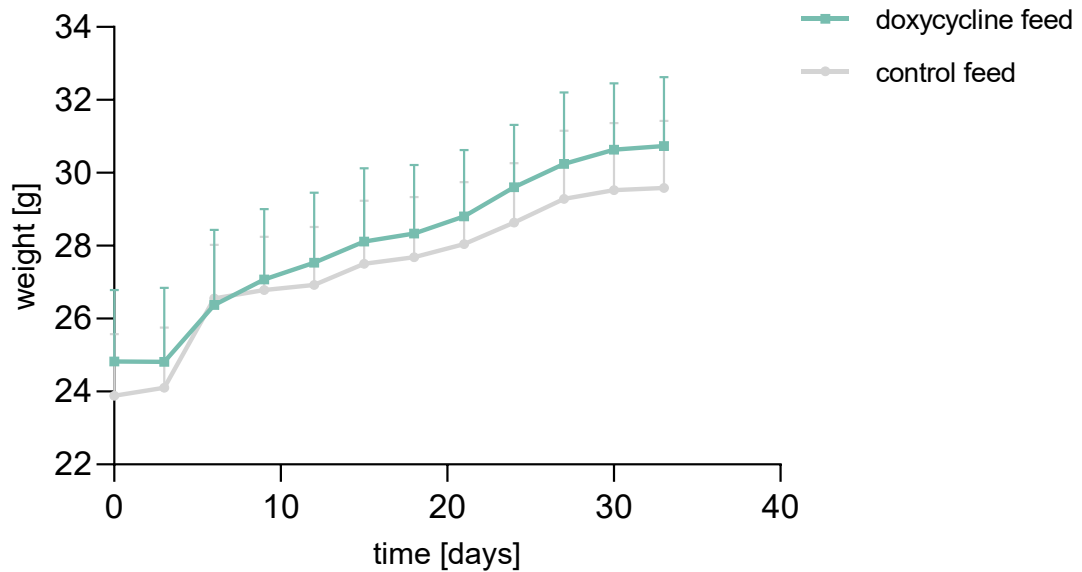


**Figure 7: Weight development** of MDA-MB-231-Tripz-200c-CMV-Luc tumor-bearing mice, fed with doxycycline-containing feed, respectively control feed. Day 0 represents the day of tumor cell inoculation. Data shown until the first animals of the control feed group were subdivided into groups for further experiments (mean + S.E.M.; n = 20 / 19 (control feed/doxycycline feed)).

To further make sure that the expression of miR-200c in presence of doxycycline in MDA-MB-231-Tripz-200c-CMV-Luc cells did not only work *in vitro* but also in the animal xenograft model, a quantitative real-time PCR analysis of 10 tumors each was performed in the doxycycline-fed as well as the control-fed group to detect the level of miR-200c expression. The real-time PCRs were carried out by Bianca Köhler, Ph.D. student at the Faculty for Chemistry and Pharmacy, Ludwig Maximilian University, Munich. Results are presented in **Figure 8** and reveal that, except for 1 animal, doxycycline induction of miR-200c expression worked well in the implanted tumors of doxycycline-fed mice.

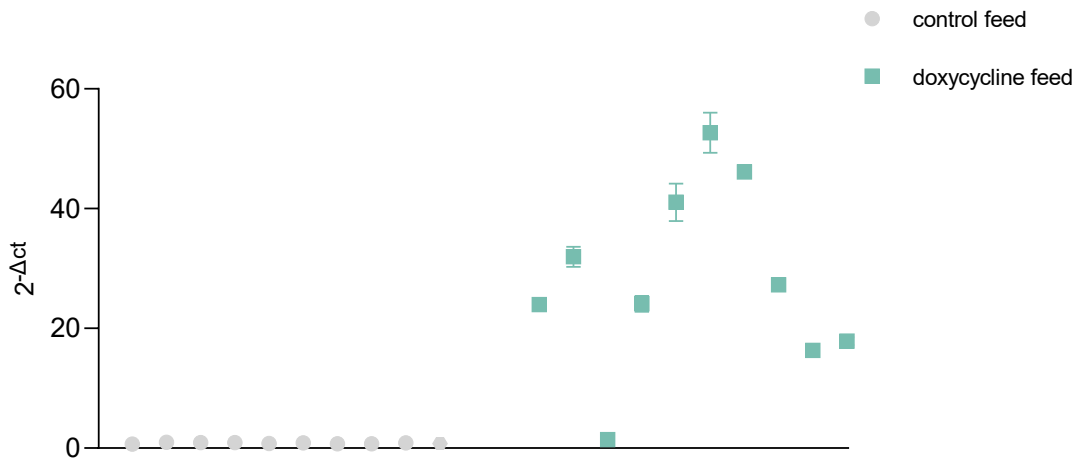


**Figure 8: miR-200c expression** of MDA-MB-231-Tripz-200c-CMV-Luc tumors in mice, fed with doxycycline-containing feed for miR-200c induction, respectively control feed. Data provided by Bianca Köhler, Ph.D. student at the Faculty for Chemistry and Pharmacy, Ludwig Maximilian University, Munich.

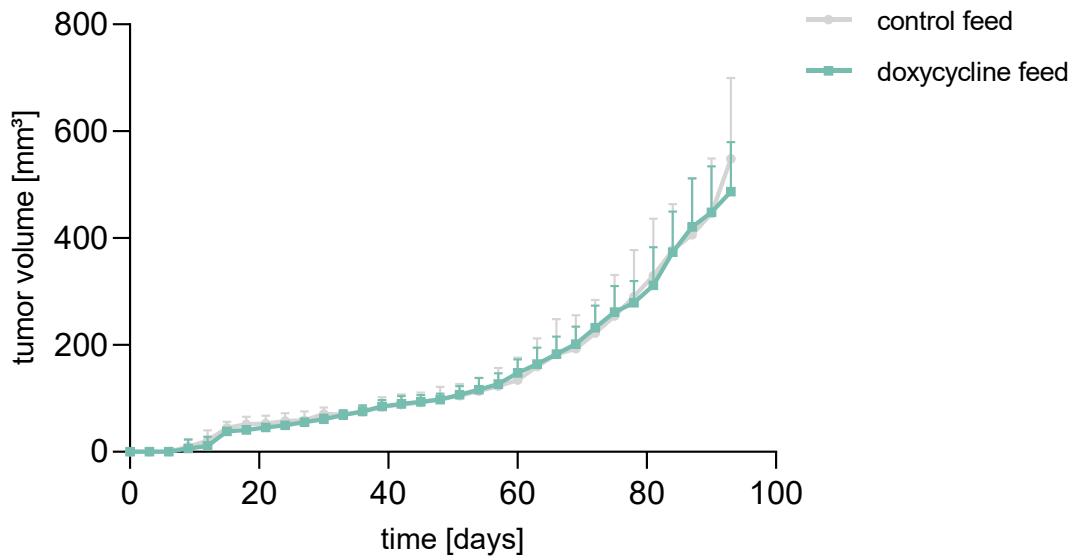
To conclude, the endogenous miR-200c expression had a significant effect on inhibiting tumorigenesis and thus resulted in a strongly delayed or fully suppressed tumor growth. According to the similar weight development of both groups, risen miR-200c levels or the doxycycline feed itself did not affect the health status of mice. Additionally, the induction of miR-200c via doxycycline feed in MDA-MB-231-Tripz-200c-CMV-Luc tumor-bearing mice was approved.

## 2 Influence of doxycycline on tumor growth

To directly trace emerged phenomena back to an increased miR-200c expression as a cause, an experiment with MDA-MB-231-Tripz-Ctrl-CMV-Luc cells was performed. As this cell line is similar to MDA-MB-231-Tripz-200c-CMV-Luc cells but does not express miR-200c while being exposed to doxycycline, possible alterations of tumorigenesis and tumor development of MDA-MB-231-Tripz-Ctrl-CMV-Luc cells could directly be linked to an impact of doxycycline itself. Therefore, tumor formation and tumor growth of 12 MDA-MB-231-Tripz-Ctrl-CMV-Luc tumor-bearing animals receiving permanently

either 625 mg/kg doxycycline-containing feed or control feed were compared. Doxycycline respectively control feed was fed permanently from 7 days prior to tumor cell inoculation. Tumors were observed respectively measured daily. **Figure 9A** represents a depiction of tumor growth in both groups until the first animals of the respective groups were euthanized. The similar curves with only slight, non-significant differences indicate that doxycycline itself does not influence tumor growth. As one animal of the control group showed an abnormally progressive and extremely proliferating tumor growth (see **Figure 9B**) it was not considered in the comparison.

A)



B)

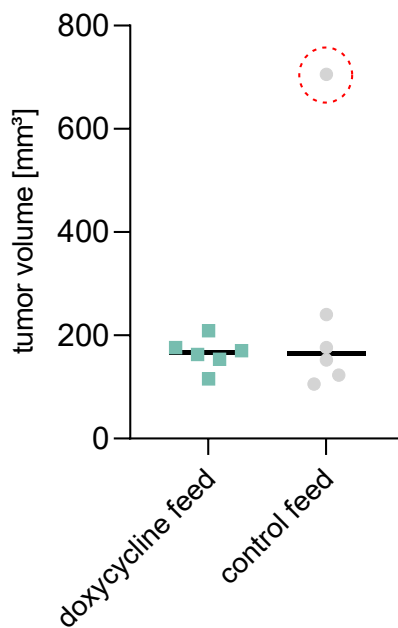


**Figure 9: Tumor growth** of MDA-MB-231-Tripz-Ctrl-CMV-Luc tumor-bearing mice, fed with doxycycline-containing feed, respectively control feed. **A)** Tumor growth of groups throughout the experiment. Day 0 represents the day of tumor cell inoculation. Data shown until the first animals of the respective groups were euthanized (mean + S.E.M.; n = 5/6 (control feed/doxycycline feed)). **B)** Comparison of tumor sizes on day 63 after tumor cell inoculation. The red circle indicates the animal that was not considered in Figure 9A.

As a result of this experiment, it can be stated that differences in tumor growth between doxycycline-fed mice and control mice in previous and all following experiments can highly likely be connected with an altered miR-200c expression as a cause.

### 3 Intratumoral application of polyplexes

The significant differences between doxycycline-induced miR-200c expressing MDA-MB-231-Tripz-200c-CMV-Luc tumors and those that did not express miR-200c paved the path for further *in vivo* delivery experiments and towards the development of new RNAi therapeutics.

For an efficient nucleic acid delivery, our working group resorts to a library of over 1500 sequence-defined oligomers as possible carriers. As **1214** turned out to be an effective candidate for siRNA delivery *in vivo* [108], we decided to utilize it for the delivery of the similarly structured miR-200c. As mentioned above, MDA-MB-231 cells are expressing the HA susceptible CD44 receptor, which is why the surface of **1214** + miR-200c was modified with 0.1 equivalents of HA-DBCO for efficient targeting and also for shielding functions.

After inoculation of MDA-MB-231-Tripz-200c-CMV-Luc tumors, 20 mice were randomly divided into 2 groups of 10 animals to receive either **1214** + miR-200c + 0.1 equiv. HA-DBCO or **1214** + siCtrl + 0.1 equiv. HA-DBCO as a control. Intratumoral injections started as soon as tumors were slightly visible and were performed twice weekly, thus, mice were injected equally on days 23, 27, 30, 34, 37, 41, and 44 after tumor inoculation. **Figure 10** represents the comparison of tumor growth in both groups until the first animals of the respective groups were euthanized. From day 10 to day 18 after the first intratumoral injection, siCtrl injected animals showed slightly larger tumors in comparison to miR-200c injected mice.

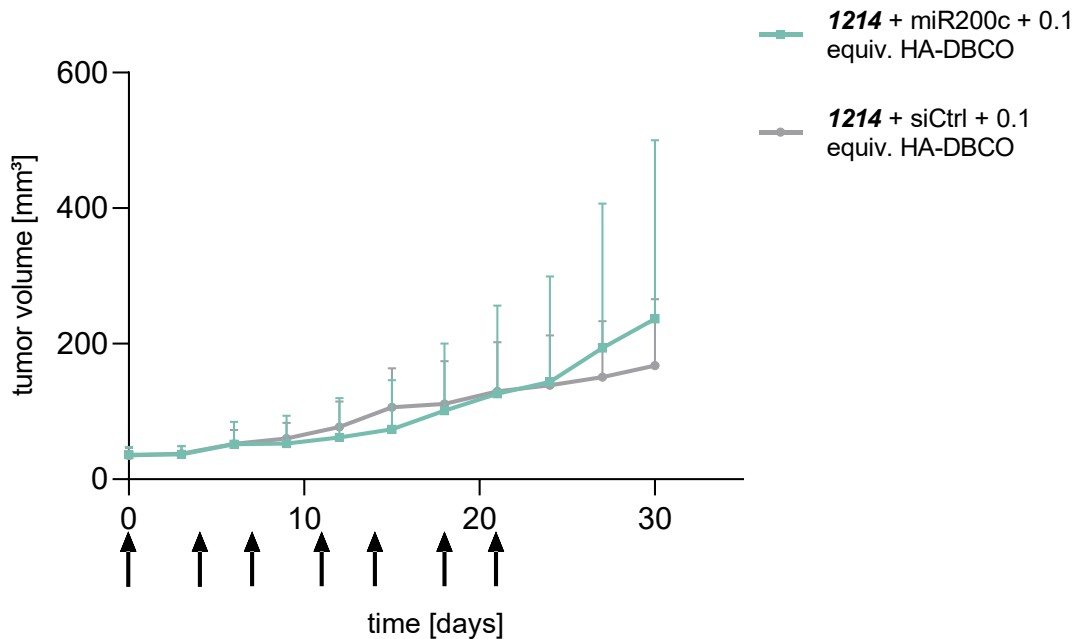


**Figure 10: Tumor growth** of MDA-MB-231-Tripz-200c-CMV-Luc tumor-bearing mice, i.t. injected with **1214** + miR-200c + 0.1 equiv. HA-DBCO, respectively **1214** + siCtrl + 0.1 equiv. HA-DBCO. Black arrows represent intratumoral injections. Day 0 represents the day of the first injection. Data shown until the first animals of the respective groups were euthanized (mean + S.E.M.; n = 10; differences are not significant).

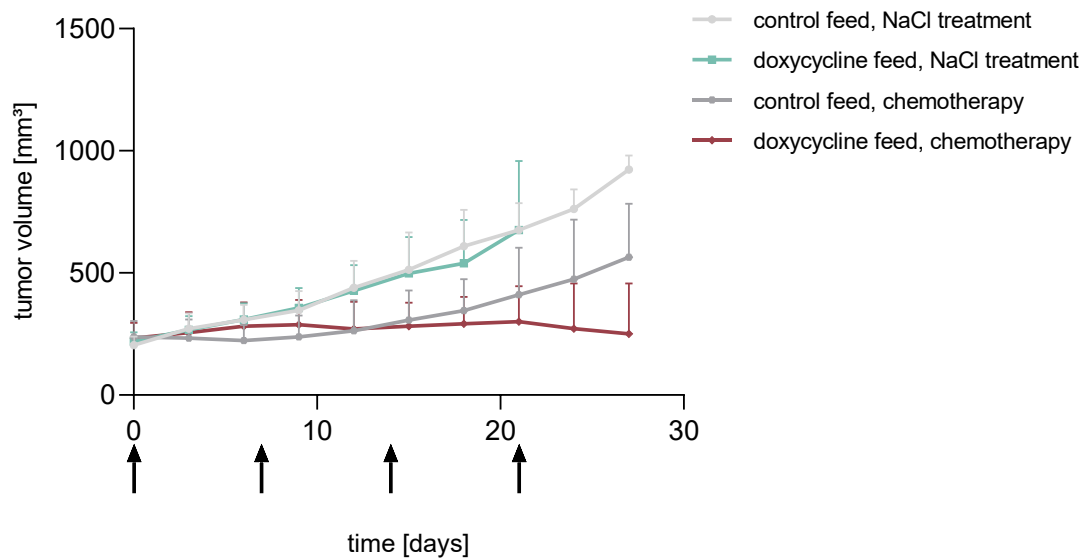
As the differences between both groups are not significant, to conclude, intratumoral injections of miR-200c polyplexes did not show a decisive effect on tumor growth.

#### 4 Antitumoral effects of miR-200c and doxorubicin

As various *in vitro* studies revealed, an increased miR-200c expression is strongly connected to a higher susceptibility to the chemotherapeutic agent doxorubicin. *Vice versa*, cells with downregulated miR-200c show significantly higher chemoresistance. As all experiments of our working group were performed *in vitro*, two separate *in vivo* experiments investigating the effects of doxycycline-induced miR-200c expression in combination with intravenous chemotherapy were conducted within this thesis.

For the first experiment, 20 mice of the tumorigenesis experiment 3.2.1 were randomly chosen when their tumors had reached a volume of 200 mm<sup>3</sup>. Until that day, mice had been receiving either doxycycline feed or control feed permanently from 7 days prior to inoculation of MDA-MB-231-Tripz-200c-CMV-Luc cells. 10 mice that had been receiving doxycycline feed for miR-200c induction were split into 2 groups receiving either chemotherapeutic treatment with doxorubicin or a NaCl treatment as a control. 10 further mice of the control-fed group were also split into 5 animals each, undergoing the same treatments. **Figure 11A** depicts the tumor growing behavior of the four groups from the first day of treatment until the first animals of the respective groups were euthanized. Whereas the control-fed group with NaCl treatment showed the largest tumors, also the doxycycline-fed group with NaCl treatment exhibited continuous tumor growth. Significant differences could be found between the two chemotherapeutic groups: while tumors started re-growing with the second doxorubicin injection in control-fed mice, doxycycline-fed mice maintained tumor size levels or even decreased them. **Figure 11B** shows a comparison between both chemotherapy groups on day 28 after the first treatment and emphasizes the suppressing effect of miR-200c on chemoresistance. With a mean volume of 565 mm<sup>3</sup>, control-fed animals reveal a more than doubled volume of doxycycline-fed animals which expose a mean of 240 mm<sup>3</sup>.

A)



B)

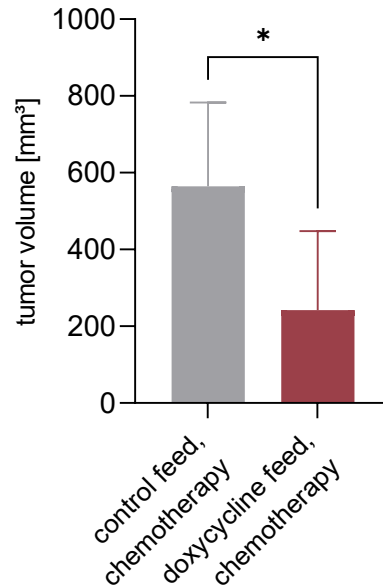
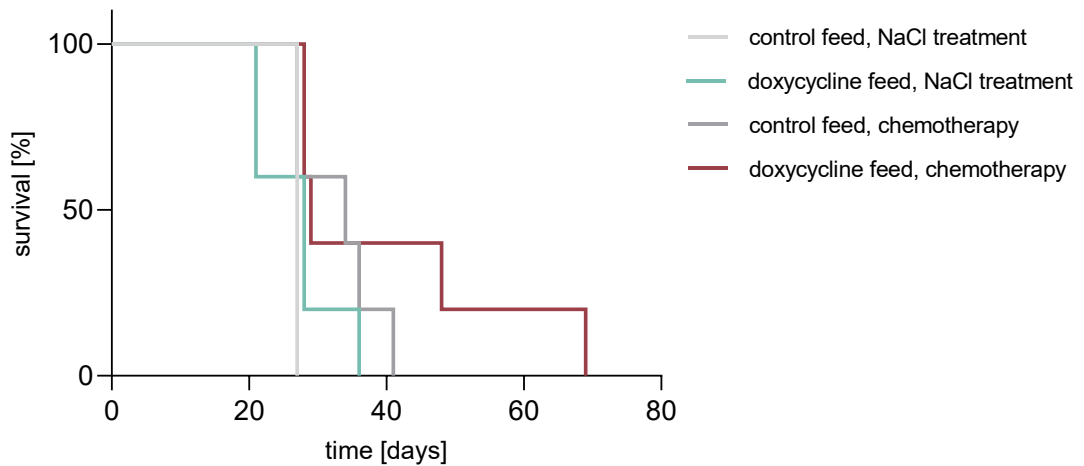


**Figure 11: Tumor growth** of MDA-MB-231-Tripz-200c-CMV-Luc tumor-bearing mice, fed with doxycycline-containing feed for miR-200c induction, respectively control feed and receiving i.v. either NaCl or 5 mg/kg doxorubicin. **A)** Tumor growth of groups throughout the experiment. Day 0 represents the day of the first treatment. Data shown until the first animals of the respective groups were euthanized. Black arrows indicate the treatments (mean + S.E.M.; n = 5) **B)** Comparison of tumor sizes of both doxycycline-fed groups on day 28 after first treatment (mean + S.E.M.; n = 5; \*p < 0.05).

To compare the survival rates of animals, a Kaplan-Meier survival analysis was performed. **Figure 12** provides an overview of the survival of mice in the four different groups. While the mean survival of both NaCl treated groups was 27 days, the chemotherapy group with the NaCl control treatment survived on average 33 days. The chemotherapy group that was fed with doxycycline feed showed the longest mean survival of 40 days. In contrast to the other groups, none of the latter animals was euthanized for its tumor size but for other reasons like weight loss or automutilation. Differences between specific groups were not significant.

A)



B)

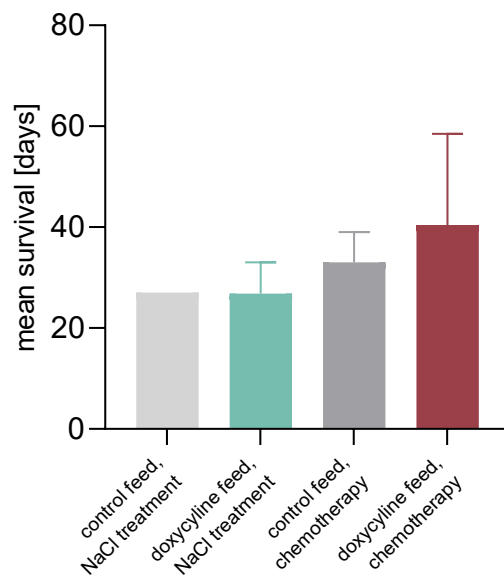


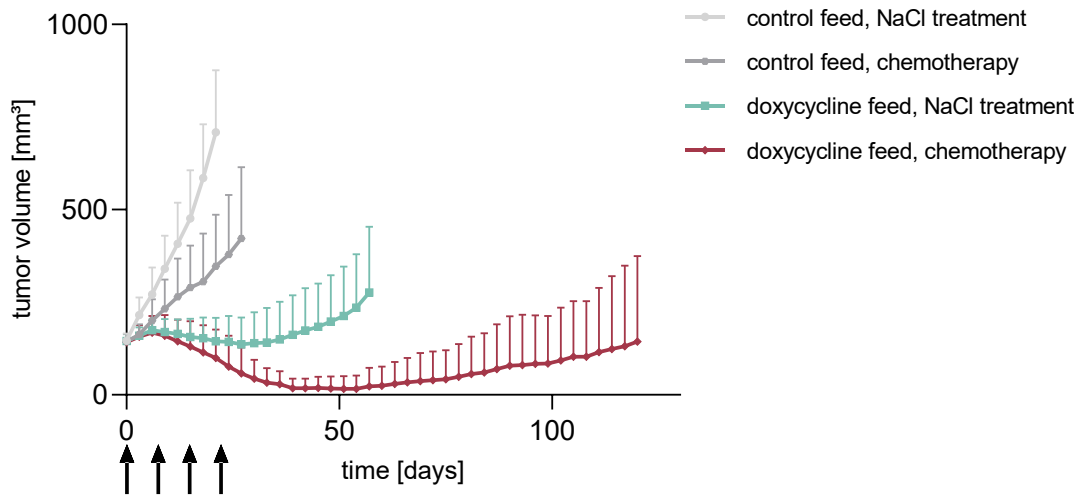
**Figure 12: Survival** of MDA-MB-231-Tripz-200c-CMV-Luc tumor-bearing mice. **A)** Kaplan-Meier survival analysis of mice fed with control respectively doxycycline-containing feed for miR-200c induction and receiving i.v. either NaCl or 5 mg/kg doxorubicin (n = 5). **B)** Mean survival of indicated groups (mean + S.E.M.; n = 5; differences are not significant).

To sum up, in contrast to its inhibiting influence on tumorigenesis in experiment 3.2.1, doxycycline-induced miR-200c expression did not show a significant antitumoral effect once tumors had reached a certain size of around 200 mm<sup>3</sup> under the permanent presence of miR-200c. In combination with chemotherapy, miR-200c-induced cells exhibited significantly smaller tumors in comparison to non-miR-200c expressing tumors, as the latter constantly increased in size after the second chemotherapeutic treatment. This phenomenon led also to a higher, but not significant mean survival of the miR-200c/chemotherapy combination group in comparison to the other three groups.

In contrast to this experiment, in a second experiment, all mice were randomly divided into 4 groups *after* their inoculated MDA-MB-231-Tripz-200c-CMV-Luc tumors had reached a certain size of around 130 mm<sup>3</sup> - 150 mm<sup>3</sup> without having been exposed to doxycycline and therefore without miR-200c expression. Once the 130 mm<sup>3</sup> - 150 mm<sup>3</sup> were reached, half of the animals continued receiving control feed and, in addition, obtained either intravenous NaCl injections or doxorubicin treatment once a week throughout 4, respectively 3 weeks, depending on their survival. The other half was switched to doxycycline feed for miR-200c induction and split into 2 groups, receiving either control or chemotherapeutic treatments as described above. Tumor sizes were measured daily and are depicted in **Figure 13A**. Data are shown until the first animals of the respective groups were euthanized, and in the case of the combinatorial doxycycline/chemotherapeutic group until the current state. The control-fed mice without chemotherapy showed a rapid and constant growing behavior until treatment day 21 with a mean volume of 710 mm<sup>3</sup>. Also, the chemotherapeutic, but doxycycline-free group showed a constant growing behavior with a mean of 420 mm<sup>3</sup> on day 28. In contrast to this, both miR-200c induced groups showed a regression in tumor development starting from 7 days after the switch to doxycycline feed. On day 58, when the first mouse of the NaCl treated doxycycline-fed animals was euthanized, the mean tumor volume of its group lay at 275 mm<sup>3</sup>. That day, the mean volume of the combinatorial miR-200c/chemotherapy group amounted

to 22 mm<sup>3</sup> and only slowly regained its 140 mm<sup>3</sup> as the start volume of treatment. **Figure 13B** compares the tumor volumes of all groups on day 21 of treatment. Whereas the control group without chemotherapy had reached a mean volume of 710 mm<sup>3</sup>, the chemotherapy mice exhibited mean volumes around 350 mm<sup>3</sup>. MiR-200c-induced tumors were the smallest with 145 mm<sup>3</sup> (NaCl treatment) respectively 100 mm<sup>3</sup> (doxorubicin).

A)



B)

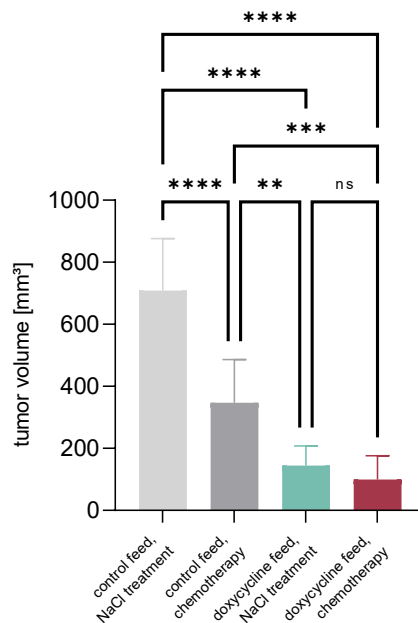


**Figure 13: Tumor growth** of MDA-MB-231-Tripz-200c-CMV-Luc tumor-bearing mice, fed doxycycline-containing feed for miR-200c induction, respectively control feed and receiving i.v. either NaCl or 5 mg/kg doxorubicin. **A)** Tumor growth of groups throughout the experiment. Day 0 represents the day of the first treatment. Black arrows indicate the treatments. Data shown until the first animals of the respective groups were euthanized. In the case of the 'doxycycline feed, chemotherapy' group, data are shown until the current state (mean + S.E.M.;  $n = 10$ ). **B)** Comparison of tumor sizes on day 21 of mice treated as indicated (mean + S.E.M.;  $n = 10$ ; \*\* $p < 0.01$ , \*\*\* $p < 0.001$ , \*\*\*\* $p < 0.0001$ , ns = not significant).

Within and after the chemotherapeutic treatments, the tumors of the combinatorial miR-200c/doxorubicin group started drastically to decrease in size until some of them were macroscopically not visible anymore and therefore amounted to a volume of 0 mm<sup>3</sup>. **Figure 14** shows the growing behavior of the specific tumors from the first day of treatment until the current state. The decrease of tumor volumes started except for one animal approximately around the second treatment. 7 animals were macroscopically tumor-free, among them one tumor recurred. At the current state, 6 animals are macroscopically tumor-free. **Figure 15** depicts the share of visible tumors in all four groups. In both doxycycline-free groups, none of the tumors decreased in size nor disappeared. One miR-200c tumor without chemotherapy decreased its volume until 0 mm<sup>3</sup>, whereas 7 combinatorial treatment animals exhibited a macroscopical tumor disappearance.

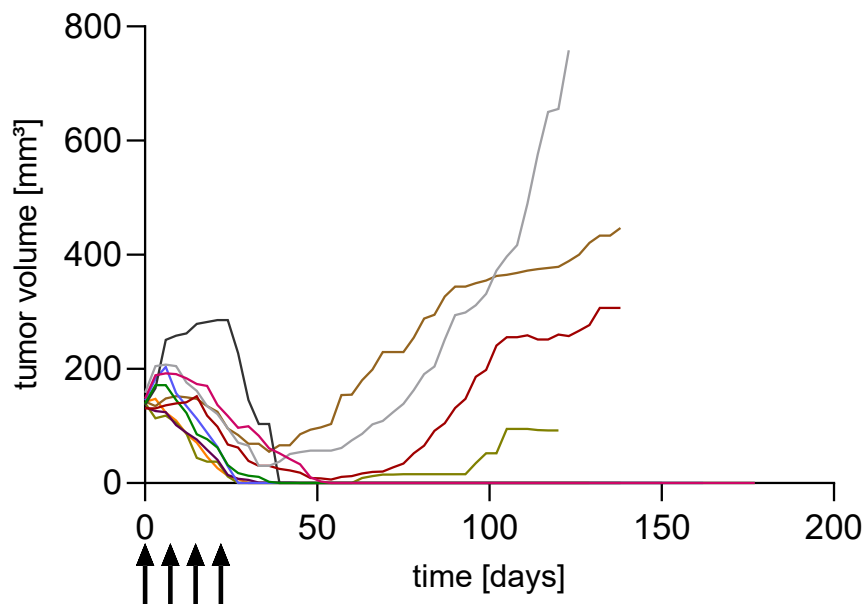


**Figure 14: Tumor growth** of single MDA-MB-231-Tripz-200c-CMV-Luc tumor-bearing mice, fed with doxycycline-containing feed for miR-200c induction and receiving 5 mg/kg doxorubicin i.v. Day 0 represents the day of the first treatment, black arrows represent the treatments. Data shown until the current state (n = 10 animals).

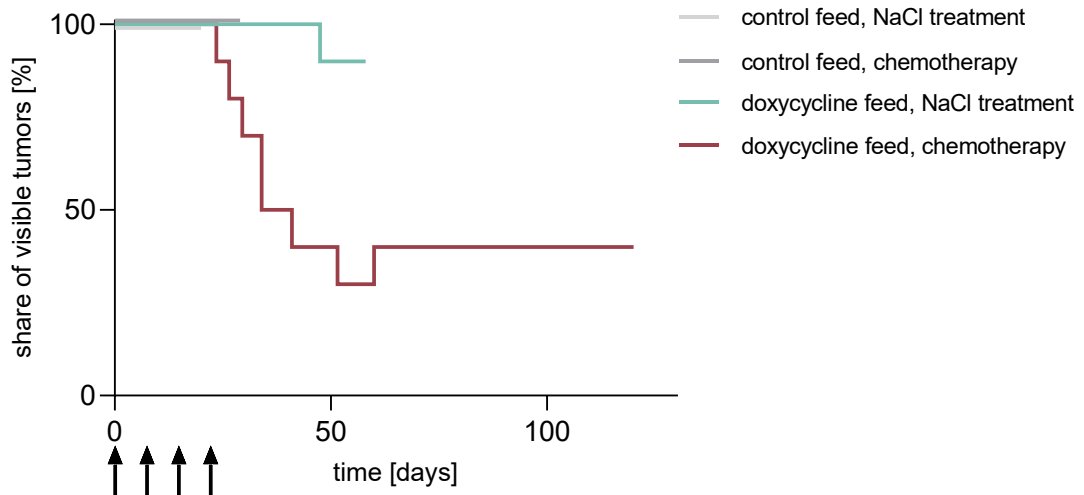


**Figure 15: Share of visible tumors** of MDA-MB-231-Tripz-200c-CMV-Luc tumor-bearing mice, fed with doxycycline-containing feed for miR-200c induction, respectively control feed and receiving i.v. either NaCl or 5 mg/kg doxorubicin. Day 0 represents the day of the first treatment. Data shown until the first animals of the respective groups were euthanized. In the case of the 'doxycycline feed, chemotherapy' group, data are shown until the current state (n = 10).

To further investigate the disappearance of tumors of the combinatorial group, *in vivo* bioimaging was performed. As MDA-MB-231-Tripz-200c-CMV-Luc cells express luciferase, possibly present but not visible remaining tumor cells could probably be detected via a luminescent signal after an intraperitoneal injection of luciferin. **Figure 16** shows luminescence of mice approx. 5 minutes after luciferin injection. Mice were imaged at two dates: once, when tumors were macroscopically no longer visible (**Figure 16A**), and once between days 120-140 after the first treatment (**Figure 16B**). One animal with a macroscopically not visible tumor showed a luminescent signal at both dates and recurrence of a visible tumor after 36 days.

A)



B)

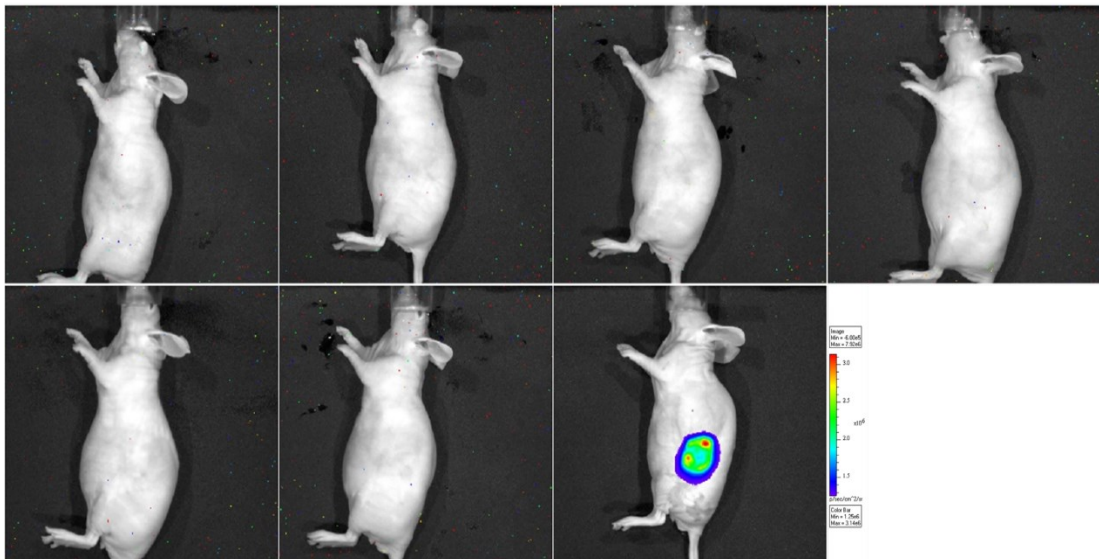
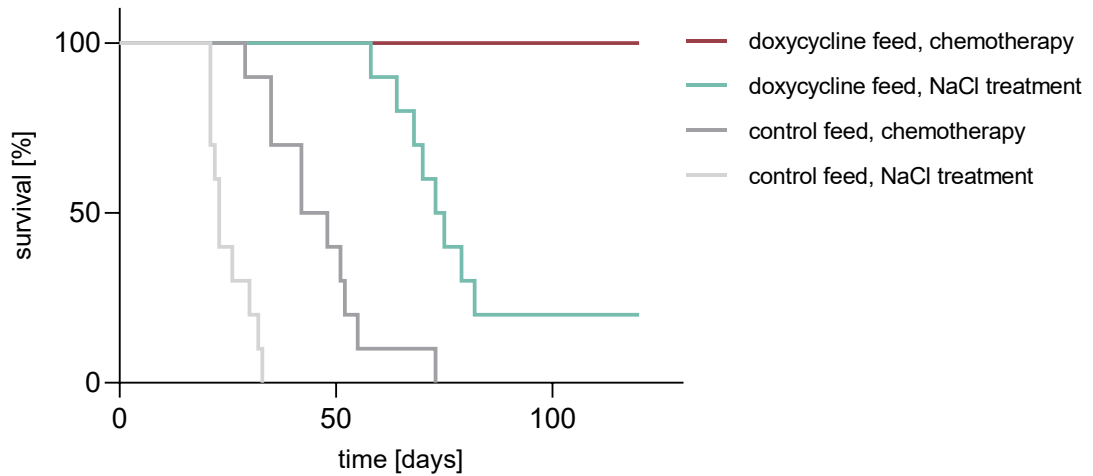


**Figure 16: Bioimaging** of 7 MDA-MB-231-Tripz-200c-CMV-Luc tumor-implanted mice fed with doxycycline-containing feed for miR-200c induction and receiving 5mg/kg doxorubicin i.v. **A)** Imaging was performed when tumors were no longer macroscopically visible. **B)** Imaging was performed between days 120 and 140 after the first treatment. The order of individual animals is the same as above.

The survival of all groups is represented in **Figures 17A and 17B**. As depicted in **Figure 17B**, animals with control feed and therefore without miR-200c expression survived on average 25 days (NaCl treatment) respectively 46 days (chemotherapy). The figure shows significant differences between the mean survivals of control-fed and doxycycline-fed animals. Among the latter, until the current state, all of the combinatorial treatment group animals are still alive and have passed 120 days of survival. Therefore, a mean survival of 120 days is set but the actual survival is higher. The NaCl-treated animals of the doxycycline-fed group exhibited a mean survival of 81 days. Also here, the value is higher due to one animal still alive that has passed 120 days and whose survival was quoted with 120 days.

A)



B)

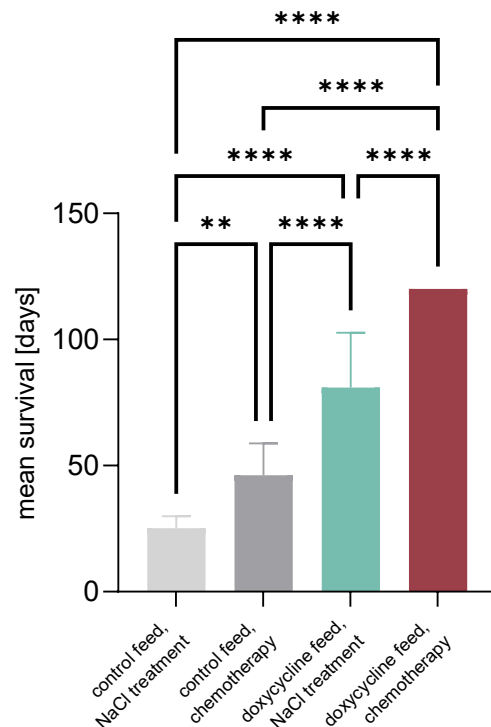


**Figure 17: Survival** of MDA-MB-231-Tripz-200c-CMV-Luc tumor-bearing mice. **A)** Kaplan-Meier survival analysis of mice fed with control feed respectively doxycycline-containing feed and receiving i.v. either NaCl or 5 mg/kg doxorubicin. Day 0 represents first day of treatment (n = 10). **B)** Mean survival of indicated groups (mean + S.E.M.; n = 10; \*\*p < 0.01, \*\*\*\*p < 0.0001).

To conclude, a transcriptionally induced miR-200c expression in MDA-MB-231-Tripz-200c-CMV-Luc tumors led to significantly repressed tumor growth with a macroscopical disappearance of the tumor in 1 out of 10 animals. MiR-200c induction in combination with chemotherapy led to even stronger reduced tumor growth and to a decrease of tumor sizes in 10 out of 10 mice. 7 out of 10 tumors completely disappeared macroscopically, among which only 1 tumor recurred. Consistent with those phenomena, miR-200c induction led to significantly higher survival in comparison to tumors without miR-200c expression. As an additional chemotherapeutic treatment seems to have cured cancer in 60 percent of the animals and strongly retarded tumor development in another 40 percent, the combination of miR-200c and chemotherapy has a significant impact on extending survival.



## IV DISCUSSION

Over the last years, our group has been working on various projects to evaluate and fathom the effects of miR-200c on tumor cells. Among other findings, we unraveled connections between miR-200c levels and expression of different migratory, detoxicating, apoptotic, or metabolic proteins [11], demonstrated the inhibiting effect of miR-200c on chemoresistance formation [35], or identified miR-200c to directly target the proto-oncogene KRAS [37]. Through the latter *in vitro* findings as well as through *in vivo* experiments in this thesis, we were inter alia able to underline the immense and significant role of miR-200c in processes of cancer and to emphasize the requirement of new and effective RNAi therapeutics. While over 60 siRNA drugs are in clinical trial progression (including the two approvals Patisiran and Givosiran), only 10 obtainable miRNA drugs have been in clinical trials with none experiencing phase III [109]. By an *in vivo* approach to deliver miR-200c with our sequence-defined oligoaminoamides, we further tried to narrow this gap but also experienced how challenging it is to overcome all obstacles of efficient delivery.

### 1 Effect of miR-200c on tumor formation and growth

By inoculating MDA-MB-231-Tripz-200c-CMV-Luc cells into mice and exposing the cells to doxycycline to attain miR-200c expression we were able to demonstrate that miR-200c significantly inhibits or even suppresses the process of tumorigenesis. Approx. 3 weeks after tumor inoculation, all 20 MDA-MB-231-Tripz-200c-CMV-Luc tumors with a lack of miR-200c were visible, whereas only one miR-200c induced tumor had appeared. 40 percent of the latter tumors did not develop at all.

Those findings emphasize on the one hand the potential of an efficient miR-200c delivery for future RNAi therapeutics, on the other hand, they highlight a

possible role of miR-200c as a prognostic marker at breast cancer diagnosis. However, the latter is still discussed controversially [110].

Multiple underlying causes for the described phenomenon can be contemplated, as various *in vitro* studies reveal. A possible central principle may be the direct targeting of the oncogene KRAS by miR-200c, detected by our working group [37]. KRAS is known to stimulate the proliferation of many cell types [111, 112] and to interfere with the cell cycle [113, 114], accentuating its role in tumorigenesis. Inversely, KRAS silencing by miR-200c was demonstrated to reduce proliferation and to alter the cell cycle of MDA-MB-436 and MDA-MB-231 cells by decreasing the number of cells in G1 phase while increasing the cell number in S phase [37]. Apart from the interaction between KRAS and miR-200c, various other targets of miR-200c may play a role by interfering with intracellular processes and therefore inhibiting cancer progression. For instance, as Ljepoja *et al.* revealed by a proteomic analysis of an *in vitro* knockout of miR-200c, multiple metabolic proteins like aspartate aminotransferase, D-3-phosphoglycerate dehydrogenase, or kynureninase were altered in their levels in the absence of miR-200c [11]. Furthermore, XIAP was identified by Ren *et al.* to be a direct target of miR-200c. XIAP, X-linked inhibitor of apoptosis, is a potent suppressor of apoptosis and can therefore stimulate cancer progression. By transfecting MDA-MB-231 cells with miR-200c, the expression of the XIAP protein was reduced, while the apoptosis ratio significantly raised in comparison to the control cells [115].

However, through the diversity and multiplicity of miR-200c targets, the suppressing effect of miR-200c on tumor progression cannot be restricted to only one origin. Future studies may be capable of further revealing the enormous potential of miR-200c in preventing tumor growth.

## 2 Delivery of miR-200c

To that day, our working group has been developing more than 1500 sequence-defined oligoaminoamides for efficient delivery of therapeutic nucleic acids into tumor tissue. For instance, we introduced siEG5-containing **1106**, which, functionalized with DBCO<sub>2</sub>-ss<sub>2</sub>-PEG<sub>24</sub>-FolA, induced a significant downregulation of EG5 mRNA expression by ~60% in tumor cells of treated L1210 tumor-bearing mice [99]. Further, in the same xenograft model, Folate-targeted and PEGylated, EG5 silencing siRNA (siEG5) containing polyplex **356**, in combination with the lipopolyplex **454**, could be shown to significantly downregulate EG5 mRNA expression by 65% [116]. HA-modified siEG5-containing **1214** could target subcutaneous Huh7 tumors and exerted 78% gene silencing after intravenous application [108].

Due to those promising results regarding siRNA delivery in Huh7 tumors, **1214** was also chosen as a carrier for the similar to siRNA structured miR-200c [104] in this thesis. As, like the Huh7 cells, also MDA-MB-231 cells express CD44 [102, 103, 117], we used HA as a passive and active targeting ligand. Thus, DBCO-amine-modified HA was functionalized with 40 µg miR-200c- (respectively 40 µg siCtrl-) containing **1214** via copper-free click reaction and injected intratumorally into MDA-MB-231-Tripz-200c-CMV-Luc tumors. During and after the 7 intratumoral injections, no significant differences between miR-200c and siCtrl-containing HA-modified **1214** polyplexes could be detected.

Possibly, a fast tumoral clearance may have prevented miR-200c from effectively entering the tumor cells. As Luo *et al.* stated in a biodistribution study, HA-modified **1214** polyplexes were cleared from the tumor tissue within 2 hours [108]. Therefore, modifications of the polyplexes must be taken into consideration for further experiments.

Another possible explanation for the similar tumor sizes of both groups may be the date of the first injection. The first injection of the polyplexes was performed

on day 23 after tumor inoculation when a tumor volume of 30 mm<sup>3</sup> to 50 mm<sup>3</sup> had been reached. This date was chosen to make sure that all tumors would grow and develop with certainty. As the intratumoral injection is restricted to a volume of 50 µl, presumably not every tumor cell could be reached by the intratumoral injections. As the non-affected, miR-200c-free tumor cells were able to grow without restriction they could have compensated for the reduced proliferation of the miR-200c-containing cells and could have led to almost unaltered tumor growth. An analysis of the mean tumor sizes in both groups three days after the last intratumoral injection might be an approach to elucidate this phenomenon: To that timepoint, the mean volume of all miR-200c injected tumors amounted to 144 mm<sup>3</sup>, whereas the siCtrl injected tumors had a similar average size of 139 mm<sup>3</sup>. Excluding all animals with a tumor size over 40 mm<sup>3</sup> at the first treatment, 6 animals in both groups are left. An examination of their tumor sizes at the same timepoint reveals a clear but non-significant ( $p = 0,09$ ) difference between the mean volumes of miR-200c injected tumors with 48 mm<sup>3</sup> in comparison to 114 mm<sup>3</sup> mean volume of siCtrl injected tumors (data not shown).

Regarding intratumoral injection, earlier starting timepoints have to be considered to achieve an efficient intracellular delivery covering more tumor cells so that tumor growth cannot be compensated by non-affected cells. Nevertheless, it is a fine line between injecting not too late and making sure that all injected tumors would have developed without an intratumoral intervention.

### 3 Antitumoral effects of miR-200c and doxorubicin

Chemoresistance to therapeutic agents is a serious challenge for cancer recurrence and is responsible for critical clinical outcomes to a large extent [118]. Especially in the metastatic setting, resistance to cytotoxic agents accounts for 90% of therapy failure [119]. The resistance to chemotherapeutic

agents can be divided into intrinsic resistance that exists already before the treatment and acquired resistance [120]. The latter develops during the treatment of tumors that were primarily sensitive and is caused by mutations occurring during treatment, respectively through other adaptive responses [120]. As Kopp *et al.* demonstrated *in vitro*, acquired resistance can arise already after only a few treatments. By treating BT474 breast cancer cells with the chemotherapeutic agent doxorubicin for three cycles, it was already possible to generate significantly more resistant cells. Further, they were able to demonstrate the connection between miR-200c levels of cells and their resistance. A significant down-regulation of miR-200c levels of the cells with less susceptibility to doxorubicin was found. *Vice versa*, an overexpression of miR-200c triggered a higher sensitivity to doxorubicin, due to downregulation of the targets TrkB and Bmi1 [35].

In this thesis, we evaluated the effects of miR-200c on doxorubicin chemotherapy and chemoresistance in two *in vivo* experiments. We demonstrated that tumors, grown under permanent expression of miR-200c, were significantly more sensitive to chemotherapy than tumors that had grown without miR-200c expression. In addition, mean survival was increased under the influence of miR-200c, though values were not significant in this first experiment. In general, the experiment shows the capability of miR-200c expression levels in breast cancer to serve as a potential prognostic marker.

In contrast to that, the second experiment underlines the potential of miR-200c for future RNAi therapeutics. On the one hand, miR-200c might serve as a therapeutic agent itself, as tumors of the experiment showed a significantly reduced growing behavior when miR-200c was induced as the only form of therapy. However, exogenous delivery of miR-200c most likely will never reach the 100% transcriptional induction of miR-200c in every tumor cell as in the current model. On the other hand, miR-200c has been demonstrated to play a tremendous role in preventing chemoresistance and improving the effectiveness of chemotherapy. Thus, tumors, having constantly grown without miR-200c influence, decreased rapidly in size when miR-200c was induced by

doxycycline feed and when a simultaneous chemotherapy was performed. 60% of animals did show a complete disappearance of their tumor without recurrence until the end of the experiment. Additionally, their survival was significantly increased.

## V SUMMARY

Cancer still ranks as one of the leading causes of death worldwide. Therapies often combine chemotherapy, surgery, and radiotherapy but frequently reach their limits, which leads to a poor prognosis of the patient. Given the hurdles those conventional therapy methods have to pass, the need for new therapeutic approaches like the delivery of therapeutic nucleic acids is undeniable.

The field of RNAi therapeutics has been extending. Patisiran and Givosiran were approved by the Food and Drug Administration as two siRNA-based therapeutics in 2018 and 2019. However, until today, no miRNA therapeutic agent has passed phase III of a clinical trial. This thesis underlines on the one hand the great potential of miR-200c as a powerful anti-cancer agent and as a supporter of preventing acquired chemoresistance. On the other hand, an attempt towards the delivery of miR-200c into tumor tissue was made.

Therefore, in the first part, the growing behavior of MDA-MB-231 breast cancer cells was analyzed *in vivo* under the presence, respectively absence of transcriptionally induced miR-200c. A significantly inhibited growing behavior was determined for the doxycycline-induced miR-200c expressing tumor cells. In a control experiment, doxycycline, as the inducer of the miR-200c expression, could be excluded as a cause of the suppressed tumor growth, thus this phenomenon could be led back to the miR-200c expression itself. The third part deals with an attempt to deliver miR-200c into MDA-MB-231 tumors and to cause a retarded tumor growth in consequence. Therefore, HA-modified **1214** miR-200c polyplexes were injected intratumorally into tumor-bearing mice several times. In comparison to the control group, the miR-200c delivered group showed no significantly altered tumor growing behavior. This reveals that the degree of exogenous delivery of miR-200c was not sufficient to affect the growth of MDA-MB-231 breast cancer, at least in absence of additional chemotherapy. At last, the effects of transcriptionally induced miR-

200c in combination with chemotherapy were evaluated. Tumors that had constantly been growing under miR-200c expression were significantly more susceptible to doxorubicin than tumors without miR-200c induction. Therefore, we disclosed miR-200c as a potential prognostic marker for cancer therapy. An induced miR-200c expression of tumors with a simultaneous chemotherapeutic treatment led to tumor disappearance without recurrence in 60% of the animals. Thus, survival was increased significantly.

To conclude, *in vivo* experiments that were performed for this thesis highlight the significant role of miR-200c as an effective therapeutic nucleic acid but also emphasize the need for research in the field of targeted delivery of miR-200c and other antitumoral agents.

## VI ZUSAMMENFASSUNG

### **MicroRNA 200c und ihre Auswirkungen auf Brustkrebs und Chemotherapie in einem Xenograftmodell**

Weltweit gilt Krebs noch immer als eine der häufigsten Todesursachen. Therapieansätze kombinieren oftmals Chemotherapie, Chirurgie und Bestrahlungstherapie, stoßen aber häufig an ihre Grenzen, was mit einer schlechten Prognose für den Patienten einhergeht. In Anbetracht der Hindernisse, die konventionelle Therapiemethoden überwinden müssen, scheint der Bedarf an neuen therapeutischen Konzepten wie dem intrazellulären Transport von therapeutischen Nukleinsäuren unabdingbar.

Das Feld um RNAi Therapeutika wächst stets. 2018 und 2019 wurden Patisiran und Givosiran von der Food and Drug Administration als zwei siRNA basierte Therapeutika zugelassen. Im Gegensatz dazu hat bis zum heutigen Tag kein miRNA Therapeutikum der Phase III der klinischen Studie standgehalten. Diese Dissertation beleuchtet einerseits das große Potential von miR-200c als maßgebendes anti-Krebs Agens und als unterstützender Faktor zur Vermeidung von erworbener Chemoresistenz. Andererseits wurde ein Ansatz zum Transport von miR-200c in Tumorgewebe verfolgt.

Hierzu wurde im ersten Teil der Dissertation das Wachstumsverhalten von MDA-MB-231 Brustkrebszellen *in vivo* unter Einfluss von miR-200c beziehungsweise in Abwesenheit von miR-200c analysiert. Hierbei wurde im Falle der von Doxyzyklin induzierten miR-200c exprimierenden Zellen ein signifikant verzögertes Wachstumsverhalten festgestellt. In einem weiteren Versuch konnte Doxyzyklin als Induktor der miR-200c Expression als Ursache für das unterdrückte Tumorwachstum ausgeschlossen und dieses Phänomen damit auf die Auswirkungen von miR-200c zurückgeführt werden. Der dritte Teil der Dissertation beschäftigt sich mit einem Versuch, miR-200c in MDA-MB-231 Tumoren zu transportieren und damit ein verzögertes

Tumorstadium auszulösen. Hierzu wurden miR-200c enthaltende, mit Hyaluronsäure modifizierte **1214**-Polyplexe wiederholt intratumoral in tumortragende Mäuse injiziert. Im Vergleich zur Kontrollgruppe wies die miR-200c injizierte Gruppe kein signifikant verändertes Tumorstadiumsverhalten auf. Es wurde deutlich, dass der Transport von miR-200c in MDA-MB-231 Brustkrebszellen für einen therapeutischen Effekt unzureichend war, und weitere Folgeexperimente wie eine Kombination mit Chemotherapie erforderlich sind. Schließlich wurden die Auswirkungen von induzierter miR-200c in Kombination mit Chemotherapie eruiert. Tumoren, die permanent unter miR-200c Expression gewachsen waren, zeigten eine signifikant größere Ansprechbarkeit auf Doxorubicin als Tumoren ohne die miR-200c Induktion. Aufgrund dessen könnte miR-200c als ein bedeutender prognostischer Faktor in der Krebstherapie in Betracht gezogen werden. Eine induzierte miR-200c Expression von Tumoren bei gleichzeitiger chemotherapeutischer Behandlung führte bis zuletzt zu einer vollständigen Rückbildung von 60% aller Tumoren. Zudem erhöhte sich die Überlebensrate signifikant.

Zusammenfassend verdeutlichen die *in vivo* Experimente, die für diese Dissertation durchgeführt wurden, die bedeutende Rolle, die miR-200c als effektive Therapeutische Nukleinsäure spielt, zeigen aber auch den Bedarf an verbessertem intratumoralen Transport von miR-200c und anderen anti-Krebs Agenzien auf.

## VII REFERENCES

1. World Health Organisation. *Cancer*. 2020 [cited 08 August 2021]; Available from: <https://www.who.int/news-room/fact-sheets/detail/cancer>.
2. Sung, H., et al., *Global Cancer Statistics 2020: GLOBOCAN Estimates of Incidence and Mortality Worldwide for 36 Cancers in 185 Countries*. CA: A Cancer Journal for Clinicians, 2021. **71**(3): p. 209-249.
3. Martínez-Jiménez, F., et al., *A compendium of mutational cancer driver genes*. Nat Rev Cancer, 2020. **20**(10): p. 555-572.
4. Tomasetti, C., L. Li, and B. Vogelstein, *Stem cell divisions, somatic mutations, cancer etiology, and cancer prevention*. Science, 2017. **355**(6331): p. 1330-1334.
5. World Health Organisation, *World Cancer Report 2020*. 2020.
6. Mattoscio, D., A. Medda, and S. Chiocca, *Human Papilloma Virus and Autophagy*. Int J Mol Sci, 2018. **19**(6): p. 1775-1787.
7. Yeldag, G., A. Rice, and A. Del Río Hernández, *Chemoresistance and the Self-Maintaining Tumor Microenvironment*. Cancers (Basel), 2018. **10**(12): p. 471-504.
8. Babaei, K., et al., *An insight of microRNAs performance in carcinogenesis and tumorigenesis; an overview of cancer therapy*. Life Sci, 2020. **240**: p. 117077-117109.
9. Mutlu, M., et al., *miR-200c: a versatile watchdog in cancer progression, EMT, and drug resistance*. J Mol Med (Berl), 2016. **94**(6): p. 629-44.
10. Achkar, N.P., D.A. Cambiagno, and P.A. Manavella, *miRNA Biogenesis: A Dynamic Pathway*. Trends Plant Sci, 2016. **21**(12): p. 1034-1044.
11. Ljepoja, B., et al., *A proteomic analysis of an in vitro knock-out of miR-200c*. Sci Rep, 2018. **8**(1): p. 6927-6942.
12. Vishnoi, A. and S. Rani, *MiRNA Biogenesis and Regulation of Diseases: An Overview*. Methods Mol Biol, 2017. **1509**: p. 1-10.
13. Li, M., et al., *MicroRNAs: control and loss of control in human physiology and disease*. World J Surg, 2009. **33**(4): p. 667-84.
14. Trang, P., J.B. Weidhaas, and F.J. Slack, *MicroRNAs as potential cancer therapeutics*. Oncogene, 2008. **27** (2): p. 552-557.
15. Regazzi, R., *MicroRNAs as therapeutic targets for the treatment of diabetes mellitus and its complications*. Expert Opin Ther Targets, 2018. **22**(2): p. 153-160.
16. Wojciechowska, A., A. Braniewska, and K. Kozar-Kamińska, *MicroRNA in cardiovascular biology and disease*. Adv Clin Exp Med, 2017. **26**(5): p. 865-874.
17. Lin, S. and R.I. Gregory, *MicroRNA biogenesis pathways in cancer*. Nat Rev Cancer, 2015. **15**(6): p. 321-33.
18. Michlewski, G. and J.F. Cáceres, *Post-transcriptional control of miRNA biogenesis*. Rna, 2019. **25**(1): p. 1-16.

19. Olejniczak, M., A. Kotowska-Zimmer, and W. Krzyzosiak, *Stress-induced changes in miRNA biogenesis and functioning*. Cell Mol Life Sci, 2018. **75**(2): p. 177-191.
20. Baumjohann, D. and K.M. Ansel, *MicroRNA-mediated regulation of T helper cell differentiation and plasticity*. Nat Rev Immunol, 2013. **13**(9): p. 666-78.
21. Krol, J., I. Loedige, and W. Filipowicz, *The widespread regulation of microRNA biogenesis, function and decay*. Nat Rev Genet, 2010. **11**(9): p. 597-610.
22. Fabian, M.R. and N. Sonenberg, *The mechanics of miRNA-mediated gene silencing: a look under the hood of miRISC*. Nat Struct Mol Biol, 2012. **19**(6): p. 586-93.
23. Rottiers, V. and A.M. Näär, *MicroRNAs in metabolism and metabolic disorders*. Nat Rev Mol Cell Biol, 2012. **13**(4): p. 239-50.
24. Romaine, S.P., et al., *MicroRNAs in cardiovascular disease: an introduction for clinicians*. Heart, 2015. **101**(12): p. 921-8.
25. da Costa Martins, P.A., et al., *Conditional dicer gene deletion in the postnatal myocardium provokes spontaneous cardiac remodeling*. Circulation, 2008. **118**(15): p. 1567-76.
26. Andreeva, K. and N.G.F. Cooper, *MicroRNAs in the Neural Retina*. International Journal of Genomics, 2014. **2014**(1): p. 897-911.
27. Cao, T. and X.C. Zhen, *Dysregulation of miRNA and its potential therapeutic application in schizophrenia*. CNS Neurosci Ther, 2018. **24**(7): p. 586-597.
28. Saliminejad, K., et al., *An overview of microRNAs: Biology, functions, therapeutics, and analysis methods*. J Cell Physiol, 2019. **234**(5): p. 5451-5465.
29. Kabekkodu, S.P., et al., *Clustered miRNAs and their role in biological functions and diseases*. Biol Rev Camb Philos Soc, 2018. **93**(4): p. 1955-1986.
30. Huang, W., *MicroRNAs: Biomarkers, Diagnostics, and Therapeutics*. Methods Mol Biol, 2017. **1617**(1): p. 57-67.
31. Lee, Y.S. and A. Dutta, *MicroRNAs in cancer*. Annu Rev Pathol, 2009. **4**(1): p. 199-227.
32. Iorio, M.V., et al., *MicroRNA gene expression deregulation in human breast cancer*. Cancer Res, 2005. **65**(16): p. 7065-70.
33. Ciafrè, S.A., et al., *Extensive modulation of a set of microRNAs in primary glioblastoma*. Biochem Biophys Res Commun, 2005. **334**(4): p. 1351-8.
34. Huang, G.L., et al., *MiR-200 family and cancer: From a meta-analysis view*. Mol Aspects Med, 2019. **70**(1): p. 57-71.
35. Kopp, F., et al., *miR-200c sensitizes breast cancer cells to doxorubicin treatment by decreasing TrkB and Bmi1 expression*. PLoS One, 2012. **7**(11): p. 50469-50480.
36. Howe, E.N., D.R. Cochrane, and J.K. Richer, *Targets of miR-200c mediate suppression of cell motility and anoikis resistance*. Breast Cancer Res, 2011. **13**(2): p. 45-60.
37. Kopp, F., E. Wagner, and A. Roidl, *The proto-oncogene KRAS is targeted by miR-200c*. Oncotarget, 2014. **5**(1): p. 185-95.

38. Liu, P., Y. Wang, and X. Li, *Targeting the untargetable KRAS in cancer therapy*. Acta Pharm Sin B, 2019. **9**(5): p. 871-879.
39. Lamouille, S., J. Xu, and R. Derynck, *Molecular mechanisms of epithelial-mesenchymal transition*. Nat Rev Mol Cell Biol, 2014. **15**(3): p. 178-96.
40. Moussa, R.A., E.Z.I. Khalil, and A.I. Ali, *Prognostic Role of Epithelial-Mesenchymal Transition Markers "E-Cadherin,  $\beta$ -Catenin, ZEB1, ZEB2 and p63" in Bladder Carcinoma*. World J Oncol, 2019. **10**(6): p. 199-217.
41. Nourmohammadi, B., et al., *Expression of miR-9 and miR-200c, ZEB1, ZEB2 and E-cadherin in Non-Small Cell Lung Cancers in Iran*. Asian Pac J Cancer Prev, 2019. **20**(6): p. 1633-1639.
42. Kim, E.J., et al., *QKI, a miR-200 target gene, suppresses epithelial-to-mesenchymal transition and tumor growth*. Int J Cancer, 2019. **145**(6): p. 1585-1595.
43. Müller, K., et al., *EGF receptor targeted lipo-oligocation polyplexes for antitumoral siRNA and miRNA delivery*. Nanotechnology, 2016. **27**(46): p. 464001-4640017.
44. Sommer, D., et al., *TALEN-mediated genome engineering to generate targeted mice*. Chromosome Res, 2015. **23**(1): p. 43-55.
45. Ljepoja, B., et al., *Inducible microRNA-200c decreases motility of breast cancer cells and reduces filamin A*. PLoS One, 2019. **14**(11): p. 4314-4332.
46. Lombaerts, M., et al., *E-cadherin transcriptional downregulation by promoter methylation but not mutation is related to epithelial-to-mesenchymal transition in breast cancer cell lines*. Br J Cancer, 2006. **94**(5): p. 661-71.
47. Chao, Y.L., C.R. Shepard, and A. Wells, *Breast carcinoma cells re-express E-cadherin during mesenchymal to epithelial reverting transition*. Mol Cancer, 2010. **9**(1): p. 179-197.
48. Sun, P., et al., *MicroRNA-based therapeutics in central nervous system injuries*. J Cereb Blood Flow Metab, 2018. **38**(7): p. 1125-1148.
49. Bonneau, E., et al., *How close are miRNAs from clinical practice? A perspective on the diagnostic and therapeutic market*. Eijfcc, 2019. **30**(2): p. 114-127.
50. Rupaimoole, R., et al., *miRNA Deregulation in Cancer Cells and the Tumor Microenvironment*. Cancer Discov, 2016. **6**(3): p. 235-46.
51. Ling, H., M. Fabbri, and G.A. Calin, *MicroRNAs and other non-coding RNAs as targets for anticancer drug development*. Nat Rev Drug Discov, 2013. **12**(11): p. 847-65.
52. Haussecker, D., *Current issues of RNAi therapeutics delivery and development*. J Control Release, 2014. **195**(8): p. 49-54.
53. Chen, Y.H., M.S. Keiser, and B.L. Davidson, *Viral Vectors for Gene Transfer*. Curr Protoc Mouse Biol, 2018. **8**(4): p. 58-65.
54. Wei, T., et al., *Delivery of Tissue-Targeted Scalpels: Opportunities and Challenges for In Vivo CRISPR/Cas-Based Genome Editing*. ACS Nano, 2020. **14**(8): p. 9243-9262.
55. Yin, H., et al., *Non-viral vectors for gene-based therapy*. Nat Rev Genet, 2014. **15**(8): p. 541-55.

56. Felgner, P.L., et al., *Nomenclature for synthetic gene delivery systems*. Hum Gene Ther, 1997. **8**(5): p. 511-2.
57. Schaffert, D., et al., *Solid-phase synthesis of sequence-defined T-, i-, and U-shape polymers for pDNA and siRNA delivery*. Angew Chem Int Ed Engl, 2011. **50**(38): p. 8986-9.
58. Berger, S., et al., *Optimizing pDNA Lipo-polyplexes: A Balancing Act between Stability and Cargo Release*. Biomacromolecules, 2021. **22**(3): p. 1282-1296.
59. Salcher, E.E., et al., *Sequence-defined four-arm oligo(ethanamino)amides for pDNA and siRNA delivery: Impact of building blocks on efficacy*. J Control Release, 2012. **164**(3): p. 380-6.
60. Lächelt, U., et al., *Fine-tuning of proton sponges by precise diaminoethanes and histidines in pDNA polyplexes*. Nanomedicine, 2014. **10**(1): p. 35-44.
61. Klein, P.M. and E. Wagner, *Bioreducible polycations as shuttles for therapeutic nucleic acid and protein transfection*. Antioxid Redox Signal, 2014. **21**(5): p. 804-17.
62. Troiber, C., et al., *Stabilizing effect of tyrosine trimers on pDNA and siRNA polyplexes*. Biomaterials, 2013. **34**(5): p. 1624-33.
63. Fröhlich, T., et al., *Structure-activity relationships of siRNA carriers based on sequence-defined oligo (ethane amino) amides*. J Control Release, 2012. **160**(3): p. 532-41.
64. Agard, N.J., J.A. Prescher, and C.R. Bertozzi, *A strain-promoted [3 + 2] azide-alkyne cycloaddition for covalent modification of biomolecules in living systems*. J Am Chem Soc, 2004. **126**(46): p. 15046-7.
65. Klein, P.M. and E. Wagner, *Click-Shielded and Targeted Lipopolyplexes*. Methods Mol Biol, 2019. **2036**: p. 141-164.
66. Treuel, L., et al., *Protein corona - from molecular adsorption to physiological complexity*. Beilstein J Nanotechnol, 2015. **6**: p. 857-73.
67. Corbo, C., et al., *Personalized protein corona on nanoparticles and its clinical implications*. Biomater Sci, 2017. **5**(3): p. 378-387.
68. Cai, R. and C. Chen, *The Crown and the Scepter: Roles of the Protein Corona in Nanomedicine*. Adv Mater, 2019. **31**(45): p. 5740-5753.
69. Suk, J.S., et al., *PEGylation as a strategy for improving nanoparticle-based drug and gene delivery*. Adv Drug Deliv Rev, 2016. **99**: p. 28-51.
70. D'Souza A, A. and R. Shegokar, *Polyethylene glycol (PEG): a versatile polymer for pharmaceutical applications*. Expert Opin Drug Deliv, 2016. **13**(9): p. 1257-75.
71. Ogris, M., et al., *PEGylated DNA/transferrin-PEI complexes: reduced interaction with blood components, extended circulation in blood and potential for systemic gene delivery*. Gene Ther, 1999. **6**(4): p. 595-605.
72. Morys, S., et al., *EGFR Targeting and Shielding of pDNA Lipopolyplexes via Bivalent Attachment of a Sequence-Defined PEG Agent*. Macromol Biosci, 2018. **18**(1): p. 203-216.
73. Rahme, K. and N. Dagher, *Chemistry Routes for Copolymer Synthesis Containing PEG for Targeting, Imaging, and Drug Delivery Purposes*. Pharmaceutics, 2019. **11**(7): p. 327-340.
74. Moreno, A., et al., *Anti-PEG Antibodies Inhibit the Anticoagulant Activity of PEGylated Aptamers*. Cell Chem Biol, 2019. **26**(5): p. 634-644.

75. Kozma, G.T., et al., *Anti-PEG antibodies: Properties, formation, testing and role in adverse immune reactions to PEGylated nano-biopharmaceuticals*. *Adv Drug Deliv Rev*, 2020. **154**: p. 163-175.
76. Abu Lila, A.S. and T. Ishida, *Anti-PEG IgM Production via a PEGylated Nanocarrier System for Nucleic Acid Delivery*. *Methods Mol Biol*, 2019. **1943**: p. 333-346.
77. Yang, Q. and S.K. Lai, *Anti-PEG immunity: emergence, characteristics, and unaddressed questions*. *Wiley Interdiscip Rev Nanomed Nanobiotechnol*, 2015. **7**(5): p. 655-77.
78. Zhang, P., et al., *Anti-PEG antibodies in the clinic: Current issues and beyond PEGylation*. *J Control Release*, 2016. **244**: p. 184-193.
79. Shimizu, T., Y. Ishima, and T. Ishida, *Induction of Anti-PEG Immune Responses by PEGylation of Proteins*. *Yakugaku Zasshi*, 2020. **140**(2): p. 163-169.
80. Yang, Y., et al., *Tumor-Targeting Anti-MicroRNA-155 Delivery Based on Biodegradable Poly(ester amine) and Hyaluronic Acid Shielding for Lung Cancer Therapy*. *Chemphyschem*, 2018. **19**(16): p. 2058-2069.
81. Novo, L., et al., *Decationized polyplexes for gene delivery*. *Expert Opin Drug Deliv*, 2015. **12**(4): p. 507-12.
82. Sudha, P.N. and M.H. Rose, *Beneficial effects of hyaluronic acid*. *Adv Food Nutr Res*, 2014. **72**: p. 137-176.
83. Cho, K., et al., *Therapeutic nanoparticles for drug delivery in cancer*. *Clin Cancer Res*, 2008. **14**(5): p. 1310-6.
84. Swain, S., et al., *Nanoparticles for Cancer Targeting: Current and Future Directions*. *Curr Drug Deliv*, 2016. **13**(8): p. 1290-1302.
85. Srinivasarao, M. and P.S. Low, *Ligand-Targeted Drug Delivery*. *Chem Rev*, 2017. **117**(19): p. 12133-12164.
86. Schrevel, M., et al., *Molecular mechanisms of epidermal growth factor receptor overexpression in patients with cervical cancer*. *Mod Pathol*, 2011. **24**(5): p. 720-8.
87. Wang, Z., *ErbB Receptors and Cancer*. *Methods Mol Biol*, 2017. **1652**: p. 3-35.
88. Scaranti, M., et al., *Exploiting the folate receptor  $\alpha$  in oncology*. *Nat Rev Clin Oncol*, 2020. **17**(6): p. 349-359.
89. Assaraf, Y.G., C.P. Leamon, and J.A. Reddy, *The folate receptor as a rational therapeutic target for personalized cancer treatment*. *Drug Resist Updat*, 2014. **17**(4-6): p. 89-95.
90. Segal, E.I. and P.S. Low, *Tumor detection using folate receptor-targeted imaging agents*. *Cancer Metastasis Rev*, 2008. **27**(4): p. 655-64.
91. Carron, P.M., et al., *Targeting the Folate Receptor: Improving Efficacy in Inorganic Medicinal Chemistry*. *Curr Med Chem*, 2018. **25**(23): p. 2675-2708.
92. Luria-Pérez, R., G. Helguera, and J.A. Rodríguez, *Antibody-mediated targeting of the transferrin receptor in cancer cells*. *Bol Med Hosp Infant Mex*, 2016. **73**(6): p. 372-379.
93. Mehra, N.K., V. Mishra, and N.K. Jain, *Receptor-based targeting of therapeutics*. *Ther Deliv*, 2013. **4**(3): p. 369-94.
94. Bayer, I.S., *Hyaluronic Acid and Controlled Release: A Review*. *Molecules*, 2020. **25**(11).

95. Mattheolabakis, G., et al., *Hyaluronic acid targeting of CD44 for cancer therapy: from receptor biology to nanomedicine*. J Drug Target, 2015. **23**(8): p. 605-18.
96. Al-Othman, N., et al., *Role of CD44 in breast cancer*. Breast Dis, 2020. **39**(1): p. 1-13.
97. Chen, C., et al., *The biology and role of CD44 in cancer progression: therapeutic implications*. J Hematol Oncol, 2018. **11**(1): p. 64-87.
98. Truebenbach, I., et al., *Sequence-Defined Oligoamide Drug Conjugates of Pretubulysin and Methotrexate for Folate Receptor Targeted Cancer Therapy*. Macromol Biosci, 2017. **17**(10): p. 520-532.
99. Klein, P.M., et al., *Folate receptor-directed orthogonal click-functionalization of siRNA lipopolyplexes for tumor cell killing in vivo*. Biomaterials, 2018. **178**: p. 630-642.
100. Zhang, W., et al., *Combination of sequence-defined oligoaminoamides with transferrin-polycation conjugates for receptor-targeted gene delivery*. J Gene Med, 2015. **17**(9): p. 161-72.
101. Truebenbach, I., et al., *Co-delivery of pretubulysin and siEG5 to EGFR overexpressing carcinoma cells*. Int J Pharm, 2019. **569**: p. 118570-118581.
102. Sheridan, C., et al., *CD44+/CD24- breast cancer cells exhibit enhanced invasive properties: an early step necessary for metastasis*. Breast Cancer Res, 2006. **8**(5): p. 59-72.
103. Asano, M., S. Tanaka, and M. Sakaguchi, *Effects of normothermic microwave irradiation on CD44(+)/CD24(-) in breast cancer MDA-MB-231 and MCF-7 cell lines*. Biosci Biotechnol Biochem, 2020. **84**(1): p. 103-110.
104. Carthew, R.W. and E.J. Sontheimer, *Origins and Mechanisms of miRNAs and siRNAs*. Cell, 2009. **136**(4): p. 642-55.
105. Janvier. *NMRI-nu Immundeficient Mouse*. 2019 [cited 20 August 2021]; Available from: [https://www.janvier-labs.com/en/fiche\\_produit/nmri-nu\\_mouse/](https://www.janvier-labs.com/en/fiche_produit/nmri-nu_mouse/).
106. Bundesministerium der Justiz und für Verbraucherschutz. *Tierschutzgesetz (TierSchG)*. 2021 [cited 20 August 2021]; Available from: <http://www.gesetze-im-internet.de/tierschg/BJNR012770972.html#BJNR012770972BJNG000103377>.
107. Faustino-Rocha, A., et al., *Estimation of rat mammary tumor volume using caliper and ultrasonography measurements*. Lab Anim (NY), 2013. **42**(6): p. 217-24.
108. Luo, J., et al., *Hyaluronate siRNA nanoparticles with positive charge display rapid attachment to tumor endothelium and penetration into tumors*. J Control Release, 2021. **329**: p. 919-933.
109. Zhang, S., et al., *The Risks of miRNA Therapeutics: In a Drug Target Perspective*. Drug Des Devel Ther, 2021. **15**: p. 721-733.
110. Huang, G.L., et al., *MiR-200 family and cancer: From a meta-analysis view*. Mol Aspects Med, 2019. **70**: p. 57-71.
111. Wang, X.Q., et al., *Oncogenic K-Ras regulates proliferation and cell junctions in lung epithelial cells through induction of cyclooxygenase-2*

- and activation of metalloproteinase-9. Mol Biol Cell, 2009. 20(3): p. 791-800.*
112. Huang, Z., et al., *PTPN2 regulates the activation of KRAS and plays a critical role in proliferation and survival of KRAS-driven cancer cells. J Biol Chem, 2020. 295(52): p. 18343-18354.*
  113. Agbunag, C. and D. Bar-Sagi, *Oncogenic K-ras drives cell cycle progression and phenotypic conversion of primary pancreatic duct epithelial cells. Cancer Res, 2004. 64(16): p. 5659-63.*
  114. Fan, J. and J.R. Bertino, *K-ras modulates the cell cycle via both positive and negative regulatory pathways. Oncogene, 1997. 14(21): p. 2595-607.*
  115. Ren, Y., et al., *microRNA-200c downregulates XIAP expression to suppress proliferation and promote apoptosis of triple-negative breast cancer cells. Mol Med Rep, 2014. 10(1): p. 315-21.*
  116. Lee, D.J., et al., *Systemic Delivery of Folate-PEG siRNA Lipopolyplexes with Enhanced Intracellular Stability for In Vivo Gene Silencing in Leukemia. Bioconjug Chem, 2017. 28(9): p. 2393-2409.*
  117. Chang, G., et al., *CD44 targets Na(+)/H(+) exchanger 1 to mediate MDA-MB-231 cells' metastasis via the regulation of ERK1/2. Br J Cancer, 2014. 110(4): p. 916-27.*
  118. Das, M. and S. Law, *Role of tumor microenvironment in cancer stem cell chemoresistance and recurrence. Int J Biochem Cell Biol, 2018. 103: p. 115-124.*
  119. Nedeljković, M. and A. Damjanović, *Mechanisms of Chemotherapy Resistance in Triple-Negative Breast Cancer-How We Can Rise to the Challenge. Cells, 2019. 8(9): p. 957-989.*
  120. Holohan, C., et al., *Cancer drug resistance: an evolving paradigm. Nat Rev Cancer, 2013. 13(10): p. 714-26.*



## VIII APPENDIX

### 1 Publications

Berger, S., Krhač Levačić, A., Hörterer, E., Wilk, U., Benli-Hoppe, T., Wang, Y., Öztürk, Ö., Luo, J., Wagner, E. *Optimizing pDNA lipo-polyplexes: A balancing act between stability and cargo release*. *Biomacromolecules*, 2021. **22**: p. 1282-1296.

Luo, J., Schmaus, J., Cui, M., Hörterer, E., Höhn, M., Däther, M., Hager, S., Benli-Hoppe, T., Peng, L., Wagner, E. *Hyaluronate siRNA nanoparticles with positive charge attach to tumor endothelium and penetrate into tumors*. *Journal of Controlled Release*, 2021. **329**: p. 919-933.

### 2 Posters

Luo, J., Schmaus, J., Cui, M., Hörterer, E., Wagner, E. *Surface charge influences the nanoparticle penetration into tumor*. CRS German Chapter Annual Meeting 2020: "Delivery and Formulation of Biologics", Munich, Germany, February 2020



## IX ACKNOWLEDGEMENTS

Zuerst möchte ich Herrn Prof. Wagner dafür danken, dass ich diese Dissertation an seinem Lehrstuhl anfertigen durfte. Vielen Dank für die stets schnelle Rückmeldung und Unterstützung und für zahlreiche Ratschläge, die mir bei der Anfertigung der Doktorarbeit eine große Hilfe waren! Danke auch für das Vertrauen in mich und für die freundliche und behagliche Atmosphäre im AK Wagner!

Ebenfalls herzlich bedanken möchte ich mich bei Herrn Prof. Dr. Eckhard Wolf für die Übernahme meiner Betreuung an der tierärztlichen Fakultät.

Wolfgang, ich kann mich gar nicht mehr erinnern, wie oft du mir bei einem Computerproblem oder wenn ein Gerät nicht funktionieren wollte aus der Patsche geholfen hast. Vielen Dank!

Markus, du sagst ja immer, ich soll nicht so oft bedanken, weil das dein Job ist, aber ein letztes Mal mach ich es trotzdem noch: Danke fürs auf unsere Tiere aufpassen, für die Arbeit an den Wochenenden, für deine spannenden Insider-Geschichten und sehr viele WhatsApp Sprachnachrichten, die mich zum Lachen gebracht haben.

Uli, ich hätte nicht gedacht, dass jemand genauso verrückt sein kann wie ich, und dann habe ich dich getroffen. Wilkbeth wurde zur Institution, hat den Biene Maia Tanz, das Speedball spielen, die Pflanzenpflege und das Matschen perfektioniert und hatte stets die besten Ideen, wie man das Germerino-Lessl Büro und den Rest des AK ein wenig aufmischen kann. Was Beth vergessen hat, hat Wilk wieder wett gemacht und umgekehrt. Danke Uli, für deinen Beitrag zu Wilkbeth, anregende Gespräche, die Radreparaturen, tolle Gesangs- und Pfeifeinlagen und natürlich auch fürs bei den Viechis helfen! Ob ich an einem neuen Arbeitsplatz überhaupt noch alleine funktionieren kann,

weiß ich noch nicht, und ich bin traurig darüber, dass ich es wohl versuchen muss.

Jana, ich kenne nicht viele Menschen, die derart hilfsbereit sind wie du. Danke dafür, dass du immer wieder angeboten hast, Aufgaben zu übernehmen, wenn es stressig für mich wurde. Du hast dich so schnell bei uns eingefunden und bist inzwischen zu einem sehr wertvollen Teil unseres Teams geworden, und das nicht nur, weil du das beste Bananenbrot der Welt backen kannst.

Und dann ist da noch der ganze Rest des AK Wagner. Der einem die Pflanzen und Fahrradhelme stiehlt, das Büro mit Weihnachtsschmuck verschandelt und der einem beim Flunkyball die Ehre raubt. Und das ganze wieder wettmacht, weil er aus den liebenswürdigsten Leuten besteht, die man sich denken kann. Leute, die Geburtstags-Überraschungsfeiern schmeißen, große Umstylings übernehmen, trösten und Hundefotos schicken, wenn es mal nicht so gut geht. Ihr Lieben, mit euch schmeckt nicht nur der Aperol und das Essen vom Codo viel besser. Ihr habt mir die Zeit am AK Wagner zu einer der schönsten überhaupt gemacht und dafür danke ich euch!